R-08-60

Premodelling of the importance of the location of the upstream hydraulic boundary of a regional flow model of the Laxemar-Simpevarp area

Site descriptive modelling SDM-Site Laxemar

Johan G Holmén, Golder Associates

March 2008

Svensk Kärnbränslehantering AB
Swedish Nuclear Fuel
and Waste Management Co
Box 250, SE-101 24 Stockholm
Tel +46 8 459 84 00

ISSN 1402-3091
SKB Rapport R-08-60

Premodelling of the importance of the location of the upstream hydraulic boundary of a regional flow model of the Laxemar-Simpevarp area

Site descriptive modelling SDM-Site Laxemar

Johan G Holmén, Golder Associates

March 2008

Keywords: Nuclear waste repository, Groundwater modelling, Boundary conditions, Water divides, Regional groundwater flow, Density dependent flow, Fractured media, Stochastic continuum.

Abstract

The location of the westernmost hydraulic boundary of a regional groundwater flow model representing the Laxemar investigation area is of importance as the regional flow of groundwater is primarily from the west towards the sea (as given by the regional topography). If the westernmost boundary condition of a regional flow model is located to close to the investigation area, the regional flow model may underestimate the magnitude of the regional groundwater flow (at the investigation area), as well as overestimate breakthrough times of flow paths from the repository area, etc.

Groundwater flows have been calculated by use of two mathematical (numerical) models:
A very large groundwater flow model, much larger than the regional flow model used in the Laxemar site description version 1.2, and a smaller flow model that is of a comparable size to the regional model used in the site description. The models are identical except for the different horizontal extensions of the models; the large model extends to the west much further than the small model. The westernmost lateral boundary of the small model is a topographic water divide approx. 7 km from the central parts of the Laxemar investigation area, and the westernmost lateral boundary of the large model is a topographic water divide approx. 40 km from the central parts of the Laxemar investigation area. In the models the lateral boundaries are defined as no-flow boundaries.

The objective of the study is to calculate and compare the groundwater flow properties at a tentative repository area at Laxemar; by use of a large flow model and a small flow model. The comparisons include the following three parameters:

- Length of flow paths from the tentative repository area.
- Advective breakthrough time for flow paths from the tentative repository area.
- Magnitude of flow at the tentative repository area.

The comparisons demonstrated the following considering the median values of the obtained distributions of flow paths properties.

The small model:

- Overestimates length of flow paths with a factor of 1.2.
- Overestimates breakthrough time of flow paths with a factor of 1.3.
- Underestimates the specific flow with a factor of 0.7.

The small model underestimates the size of the groundwater flow; the underestimation follows from the limited size of the small model and the weakly developed surface water divide used as the westernmost boundary condition of the small model. The weakly developed surface water divide is conceptually applied in the small model as a groundwater divide; and in the small model it is represented by a no-flow boundary condition. The simulation with the large model demonstrates however that the weakly developed surface water divide is not a groundwater divide for the groundwater flow at large depths.

It follows that the deep groundwater flow that passes below the weakly developed surface water divide will not be included in the small model. As this deep groundwater flow is not included in the small model, the small model will underestimate the groundwater flows at the repository area, and overestimate lengths of flow paths as well as the breakthrough times of flow paths from the repository area. The differences when comparing the flow paths properties (as calculated by the large and small models) are however not large; because the deep groundwater flow that is missing in the small model is not large.

Contents

1 Introduction and purpose

1.1 Introduction

As a part of the site description of the Laxemar subarea, groundwater flow models have been used for estimating the size and direction etc, of the groundwater flow.

The location of the westernmost boundary of a groundwater flow model representing the Laxemar-Simpevarp area is of importance as the regional flow of groundwater is primarily from the west towards the sea (as given by the regional topography). If the westernmost boundary condition of a regional flow model is located to close to the investigation area, the regional flow model may underestimate the size of the regional groundwater flow at the investigation area.

1.2 Purpose

Considering a regional flow model representing the Laxemar-Simpevarp area, the purpose of this study is to estimate how the position of the westernmost boundary condition influences:

- The calculated groundwater flow at an area representing a tentative repository located at the Laxemar investigation area.
- Calculated properties of flow paths from the tentative repository area.

In this study we have established and analysed different supraregional and regional flow models representing the Laxemar-Simpevarp area and its surroundings. These models are based on the supraregional modelling as presented in /Ericsson et al. 2006/, and on the results of the site investigations, as given in /Rhén et al. 2006/.

The purpose of the flow modelling presented in this study is solely to analyse the importance of the position of the westernmost boundary of a regional flow model.

2 Methodology and description of the studied flow system

2.1 The system analysis approach

In this study the limited part of the reality that we are investigating is called *the system*. *The model* is an idealised and simplified description of the studied system. This study is based on *the system analysis approach*. This is a method for solving complicated problems by: (i) establishing a model of the studied system, (ii) using the model for simulations which imitate the behaviour of the studied system and (iii) based on the results of the simulations, gain insight into the behaviour of the studied system.

2.2 General methodology and objectives

The objective is to calculate and compare the groundwater flow at a tentative repository area at Laxemar; for a very large groundwater flow model, much larger than the regional flow model used by /Hartley et al. 2006/ (SKB R-06-23 Site description version 1.2), as well as for a flow model that is of a comparable size to the regional model used by /Hartley et al. 2006/. The comparison regards different aspects of the groundwater flow, and based on the comparisons we will estimates how the position of the westernmost boundary condition influences the groundwater flow at the area studied.

The comparisons include the following three parameters:

- Length of flow paths from the tentative repository area.
- Advective breakthrough time for flow paths from the tentative repository area.
- Magnitude of flow at the tentative repository area.

2.3 Flow equation and computer code

The groundwater flow is calculated by use of the numerical mathematical model DarcyTools 3.0 /Svensson et al. 2004/. The established model is a mathematical description of the system studied. The description is based on a continuum approach, and it is a three dimensional description that includes time-dependent and density dependent effects.

DarcyTools 3.0 uses the finite difference method for the numerical solution of the mathematical problem. The studied domain is divided into a large number of computational cells, and these cells may be of different sizes. Properties of the system studied that are scalars (e.g. pressure, porosity, salinity etc) are defined at the centre of the cell. But direction dependent properties (e.g. hydraulic conductivity) are defined (or calculated) for the faces of the cells (the cell-walls).

In DarcyTools the mass conservation equation is formulated as follows /Svensson et al. 2004/:

$$\frac{\partial(\rho\varepsilon)}{\partial t}+\frac{\partial}{\partial x}(\rho u)+\frac{\partial}{\partial y}(\rho v)+\frac{\partial}{\partial z}(\rho w)=Q$$

ρ = *Fluid density*

ε = *Fluid porosity (effective porosity)*

u, v, w = Darcy flows (specific flows)

Q = Inflow or Outflow

The flow equations are pressure dependent and formulated in the following way /Svensson et al. 2004/:

$$\rho u = -\frac{K_x}{g}\frac{\partial p}{\partial x}$$

$$\rho v = -\frac{K_y}{g}\frac{\partial p}{\partial y}$$

$$\rho w = -\frac{K_z}{g}\frac{\partial p}{\partial z} - K_z(\rho - \rho_0)$$

g = Acceleration of gravity

p = The dynamic pressure in relation to a hydrostatical reference pressure

K_x , K_y , K_z = Hydraulic conductivity along coordinate axes

ρ_0 = Density of a reference fluid (e.g. fresh water)

In DarcyTools, the transport of salinity is handled in parallel by two different processes:

- Advection-diffusion through a continuous flow medium, as represented by the effective porosity of the cells of the computational grid.
- A diffusive exchange between the moving fluid in the computational cells and a stagnant pore-volume (non-flowing porosity). This exchange takes place on a scale smaller than the scale of the computational cells (a sub-grid process).

The equation for mass transport via advection-dispersion is formulated in the following way /Svensson et al. 2004/.

$$\frac{\partial \rho \varepsilon C}{\partial t} + \frac{\partial}{\partial x}\left(\rho u C - \rho \gamma D_x \frac{\partial C}{\partial x}\right) + \frac{\partial}{\partial y}\left(\rho v C - \rho \gamma D_y \frac{\partial C}{\partial y}\right) + \frac{\partial}{\partial z}\left(\rho w C - \rho \gamma D_z \frac{\partial C}{\partial z}\right) = Q C + Q_c$$

C = Transported mass-fraction of salt

D_x , D_y , D_z = Hydrodynamic dispersion along the coordinate axes

Q_c = Inflow or Outflow. A diffusive exchange of salt between the moving water inside the effective porosity and the stagnant fluid in the non-flowing pore-volume

γ = Compacation of the flow medium

The diffusive exchange of salt between the moving water inside the effective porosity and the stagnant fluid in the non-flowing pore-volume is modelled by use of a “multi-rate” diffusion model. This model is based on a one-dimensional “multi-rate” formulation presented in /Haggerty och Gorelick 1995/. A more detailed description is given in /Svensson et al. 2004/ and /Follin et al. 2005/.

2.4 Extension and topography of domain studied

The domain studied is bounded by regional topographic water divides. The regional topographic water divides of southern Sweden is given in Figure 2-1 (below). Three regional drainage basins are included in the large model of this study, in Figure 2-1 (below) these areas are denoted as the brown area, the light green area and the blue area.

The supraregional modelling /Ericsson et al. 2006/ included all the areas discussed above, but in addition the supraregional model also included the large Emån drainage basin (SMHI drainage basin No. 74, area: 4,472 km^2), and the small coastal near drainage basin between Emån and Virån, see Figure 2-2.

The topography of the area analysed in this study is given in Figure 2-3. Basin 1 is the Virån drainage basin (SMHI basin No. 73, area: 73,588 km^2). Basin 2 is the Marströmmen drainage basin (SMHI basin No. 72 area: 496 km^2). Basin 3 is a smaller coastal near drainage basin which has not been given any name by SMHI. The red box denotes the extension of the Oskarshamn regional investigation area.

The supraregional topography is given by the national grid RT90/RH70 ("Rikets nät") with a resolution of 50×50 m. At the regional investigation area, and somewhat outside of this area, the data from the national grid were replaced by local topographic data: The resolution of the local topographic data varies between 50×50 m and down to a resolution of 20×20 m (see Figure 3-1).

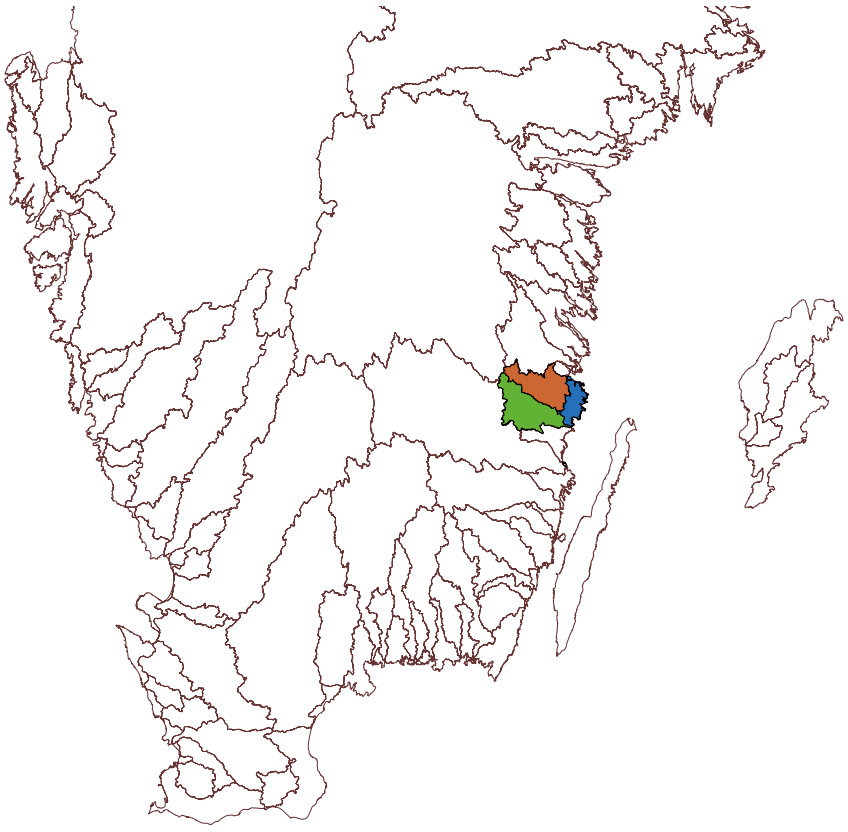

Figure 2-1. *Regional topographic surface water divides of southern Sweden. The brown area, the light green area and the blue area are included in the large mode of this study.*

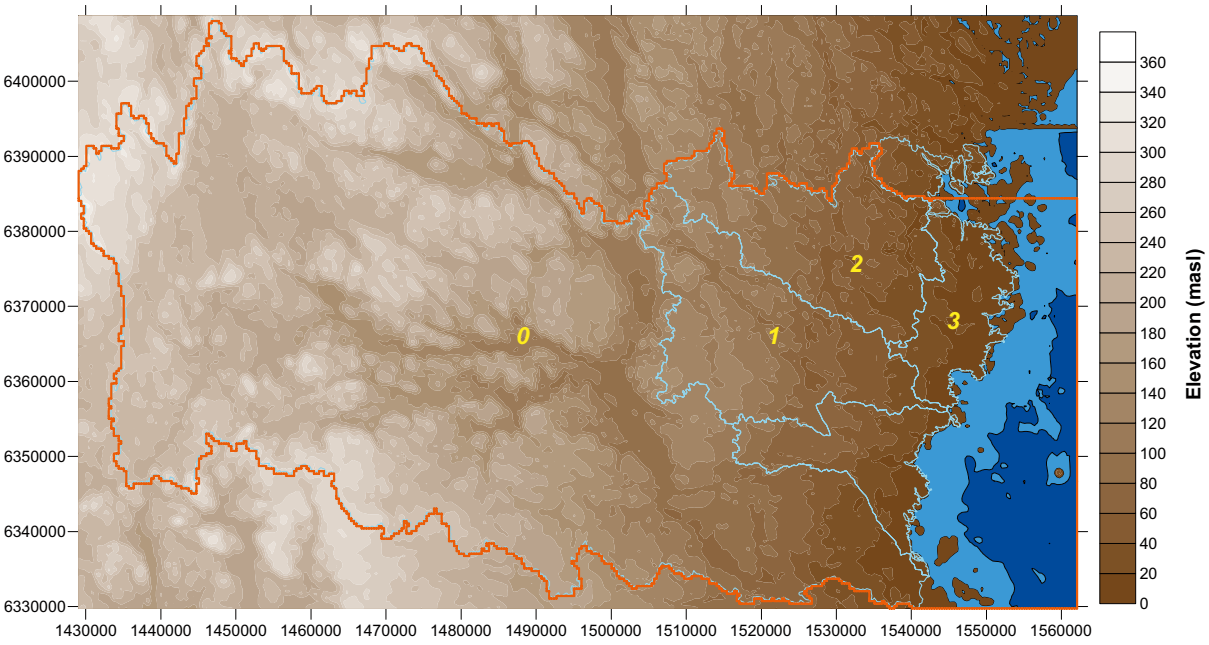

Figure 2-2. *The topography of the supraregional area. The area above was included in the supra-regional modelling /Ericsson et al. 2006/. Area 0 is the large Emån drainage basin (SMHI drainage basin No. 74, area: 4,472 km²) this area is not included in this study.*

As seen in Figure 2-2 there is a significant topographic surface water divide between Basin 0 (Emån drainage basin) and Basin 1. West of the water divide between these two drainage basins the topography forms different large heights separated by the river valleys of the Emån and Silverån rivers. East of the water divide between Basin 0 and Basin 1 the topography is on – a regional scale – gently dipping towards the sea (the Subcambrium Peneplane, see /SNA 1994/. The Emån drainage basin is not included in the established model, as it is located west of a significant topographic water divide. It is likely that this topographic water divide is an effective groundwater divide; this can be concluded from the results presented in /Ericsson et al. 2006, Figures 6-8, 6-19 and 6-20/.

Approximately 5 km to 12 km west of the shoreline there is a weakly developed topographic surface water divide between Basin 3 and Basins 1 and 2; the surface water divide is marked in Figure 2-3 with a purple line. This surface water divide is at the focus of this study.

Both west and east of the above discussed weakly developed surface water divide, the topography is gently dipping towards the sea (on a regional scale). The surface water divide is "weakly developed" as it is only a consistent surface water divide (a consistent topographic ridge) if the topography is analysed with a very fine resolution. If the topography is analysed with a resolution of e.g. 100 m (or larger), it is likely that the regional topographic gradient (gently dipping towards the sea) will come to dominate the analysis and the weakly developed surface water divide will not show up as a consistent surface water divide in such an analysis. This is discussed and analysed in more detail in Chapter 3.

A strongly developed surface water divide is a topographic ridge that dominates not only the local topography, but also the regional topography, such a structure is a consistent surface water divide even if the topography is analysed with a resolution that is not very detailed. The westernmost part of the surface water divide between Basin 0 (Emån drainage basin) and Basin 1 (see Figure 2-2) is an example of a strongly developed surface water divide.

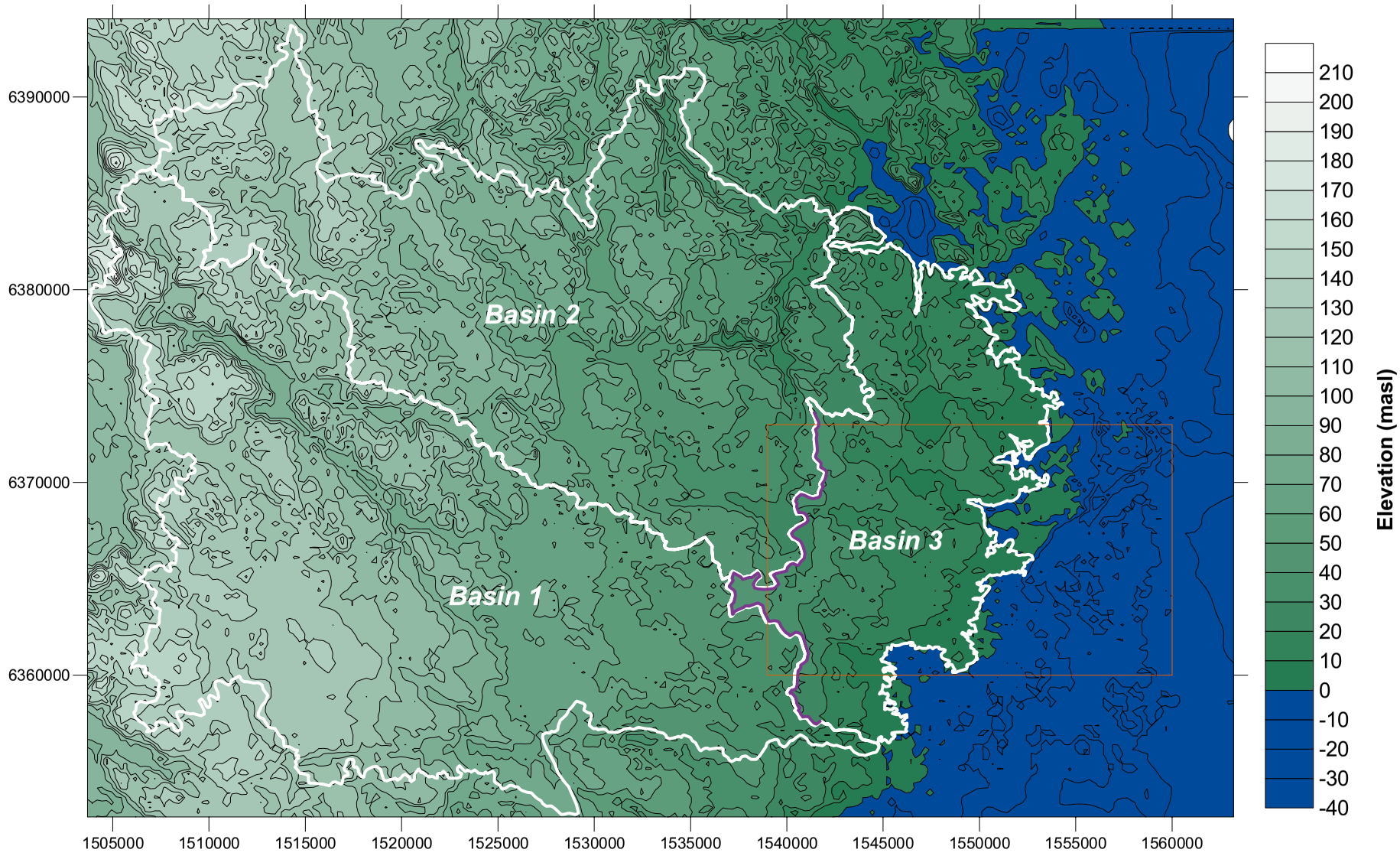

Figure 2-3. *Extension and topography of area studied. Basin 1 is the Virån drainage basin (SMHI basin No. 73, area: 588 km²). Basin 2 is the Marströmmen drainage basin (SMHI basin No. 72, area: 496 km²). Basin 3 is a smaller coastal near drainage basin which has not been given any name by SMHI. The red box denotes the extension of the Oskarshamn regional investigation area. The white lines denote regional surface water divides. The purple line denotes the weakly developed surface water divide between Basin 3 and Basins 1 and 2.*

2.5 Extension of models studied

Two models have been established: (i) the small model and (ii) the large model. The lateral extensions of these two models are given in Figure 2-4.

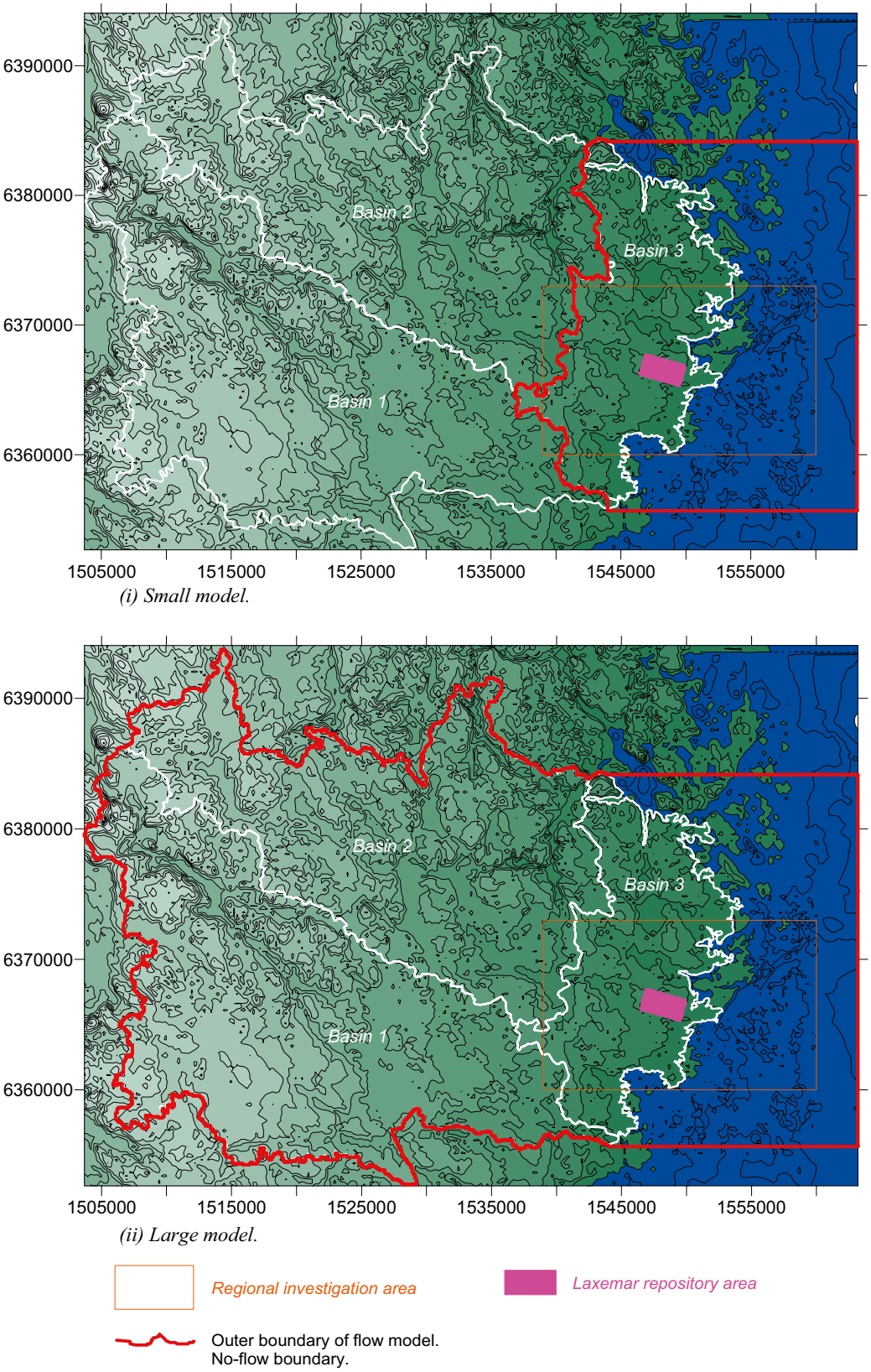

Figure 2-4. *Extension (red line) of small model (upper figure) and large model (lower figure).*

The small model has a length in the west-east direction of 19 km to 26 km, and a length in the south-north direction of approximately 29 km.

The large model has a length in the west-east direction of approximately 57 km, and a length in the south-north direction that varies between 28 km and 40 km.

To the east both the small and the large model have a large extension below the sea, the models extend beyond the regional investigation area towards the east and the minimum distance from the east boundary to the shoreline is approximately 8.5 km.

The westernmost boundary of the small model is the regional water divide between basin 3 and the two basins west of basin 3. This is also the boundary used in the regional flow model of the Laxemar site description version 1.2, see /Hartley et al. 2006/; the extension of the model used in /Hartley et al. 2006/ is presented in Figure 2-5.

The minimum distance between the central part of the local investigation area (Laxemar repository area) and the west boundary of the small model is approximately 7 km.

The westernmost boundary of the large model is the regional water divide between the large Basin 0 (Emån drainage basin) and Basins 1 and 2 (see Figure 2-2). The minimum distance between the central part of the local investigation area (Laxemar repository area) and the west boundary of the large model is approximately 40 km.

The lateral boundaries are defined as vertical and the model is defined with a base level at an elevation of –2,500 m above sea level. The upper boundary follows the topography.

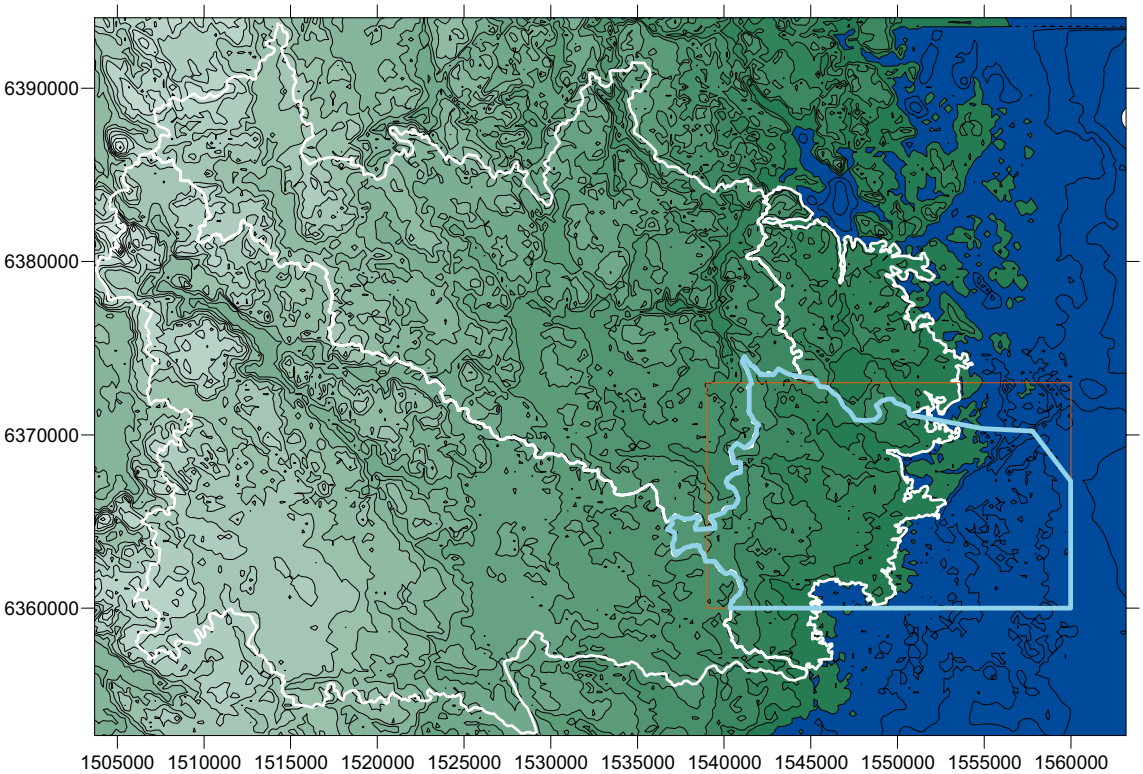

Figure 2-5. *Extension of the regional flow model of Laxemar site description version 1.2, see /Hartley et al. 2006/. The extension of the model is denoted by the thick light-blue line.*

2.6 Rock mass

2.6.1 General formulation

The rock mass is divided into different lithological units, in the same way as was done for the supraregional modelling /Ericsson et al. 2006/. The extension of the different units is based on data provided by SGU (Swedish Geological Survey), see /Ericsson et al. 2006, page 47/. The extension of the lithological units is given in Figure 2-6 (below). The different units represent different types of rock; Table 2-1 (below) presents the different rock types.

Table 2-1. The rock mass: the lithological units as defined in the model. The table below explains the codes given in Figure 2-6, above.

Lithological unit	Code
Granite, Quartz-monzonite, Syenite and metamorphic equivalents.	607
Rhyolite, Conglomerate, Sandstone.	754
Granite, Granodiorite, Quartz-monzonite, Monzonite, Syenite and metamorphic equivalents.	756
Gabbro, Diorite, Ultramafic rock and metamorphic equivalents.	757
Gabbro, Diorite, Ultramafic rock and metamorphic equivalents.	758
Mafic to intermediate volcanic and metavolcanic rocks.	767
Felsic to intermediate volcanic and metavolcanic rocks.	768
Quartzite, Meta-arkose.	771
Metagreywacke, Metasiltstone, Metasandstone, Mica-schist. Graphite- and/or sulphide-bearing schist, Paragneiss, Amphibolite intercalations.	775

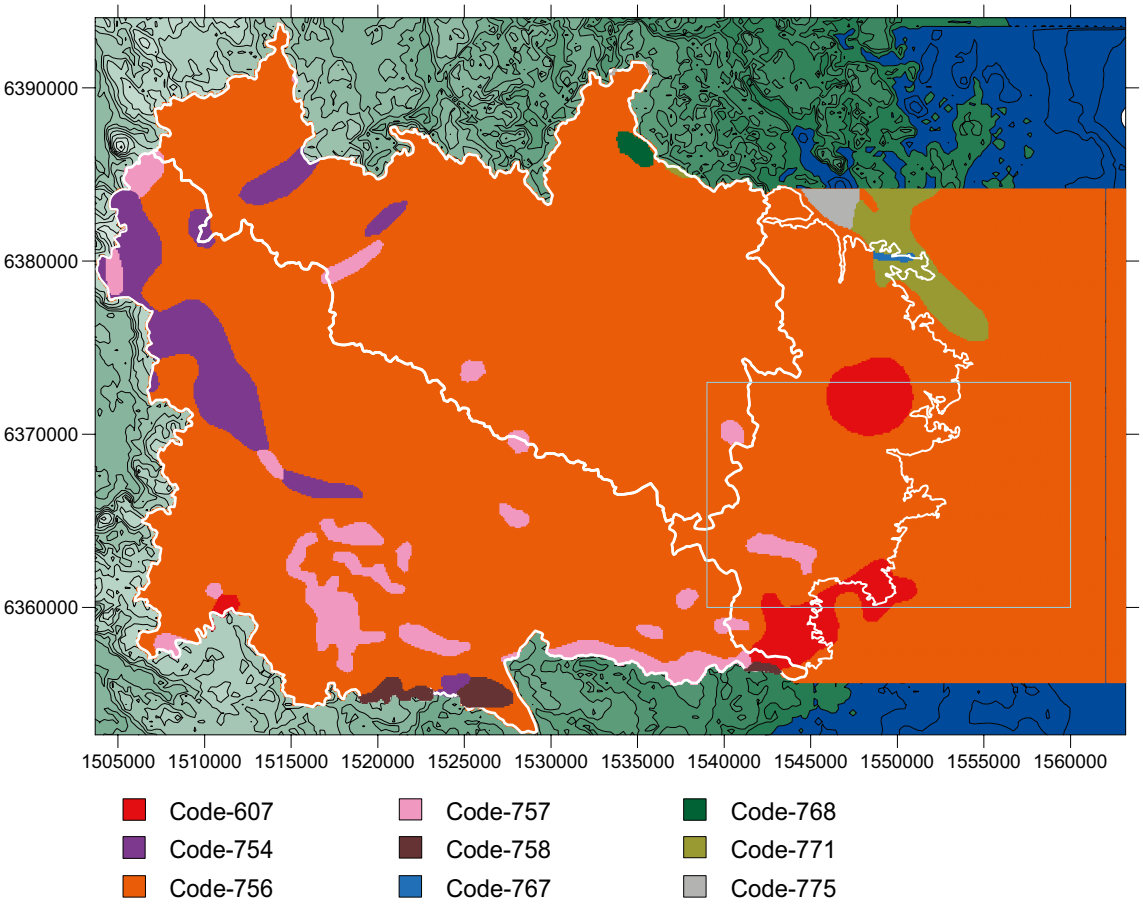

Figure 2-6. *The rock mass: the lithological units as defined in the model. The codes given in the figure above corresponds to different lithological units that are explained in Table 2-1, below.*

The values of hydraulic conductivity of the different lithological units is defined in the same way as in /Ericsson et al. 2006/, we refer to that study for a detailed description of the methodology, a short summary is however given below.

The model has been assigned conductivity values (K-values) based on the assumption that the K-values depend on lithological unit. The K-values of the different lithological units are derived from data presented by SGU in the hydrogeological maps and descriptions of Jönköpings län and Kalmar län, as well as data derived from the "Water well archive" of SGU. These K-values represent the permeability close to surface (at a depth of approximately 50–70 m). To allow for a stochastic continuum approach, a variation in permeability has also been calculated for each lithological unit, based on data obtained from the SKB site investigations, see /Ericsson et al. 2006/.

Hence, for each lithological unit we have derived a K-value representing the mean permeability close to ground surface (at an approximate depth of 60–70 m) and a standard deviation representing the variation in K-values within the lithological unit. The obtained K-values and the obtained values of standard deviation are given in below in Table 2-2.

As the model extends down to a depth of 2,500 m above sea level a depth dependency of the permeability has been introduced for each lithological unit. (This was also done in the study by /Ericsson et al. 2006/. The depth dependency is based on the results of the site investigation /Rhén et al. 2006/ (Laxemar site description version 1.2).

Above a depth of 67 m, the K-value is set as constant and equal to the K-value derived based on the SGU-data (see Table 2-2). Below a depth of 67 m the K-value decreases in line with the depth dependence observed at the site investigation /see Rhén et al. 2006/. The following equation has been used.

$d > 67\ m \rightarrow K = C\ d^{L}$

$d <= 67\ m \rightarrow K = K_{67m}$

d = Depth [m]

K = Conductivity of the rock mass (effective value in stochastic continuum formulation) [m/s]

K_{67m} *= Conductivity of the rock mass, representative values, see Table 2-2 [m/s]*

C = A coefficient selected in a way that the K-value at a depth of 67 m is equal to K_{67m}

L = –2.1838 (exponent describing the depth dependency)

Table 2-2. Properties of lithological units, as defined in /Ericsson et al. 2006, Table 2-2/.

	Properties of lithological units, based on SGU-data	
Lithological unit	**Surface near K-value [m/s]**	**Scaled standard deviation in 10Log space [m/s]**
Unit 607	1.60 E–7	1.3
Unit 754	2.36E–8	1.44
Unit 756	1.60E–7	1.3
Unit 757	2.60E–8	0.94
Unit 758	4.83E–8	1.37
Unit 767	4.00E–8	1.12
Unit 768	5.90E–8	1.17
Unit 771	3.80E–7	1.26
Unit 775	2.84E–8	1.20

The resulting depth dependencies of the lithological units are given in Figure 2-7.

The rock mass of the lithological units are defined as heterogeneous by use of a stochastic continuum approach. The methodology for the stochastic continuum approach is discussed in Appendix A.

The definitions of the properties of the rock mass of the established model are similar to that of Case 8A s2 in /Ericsson et al. 2006/.

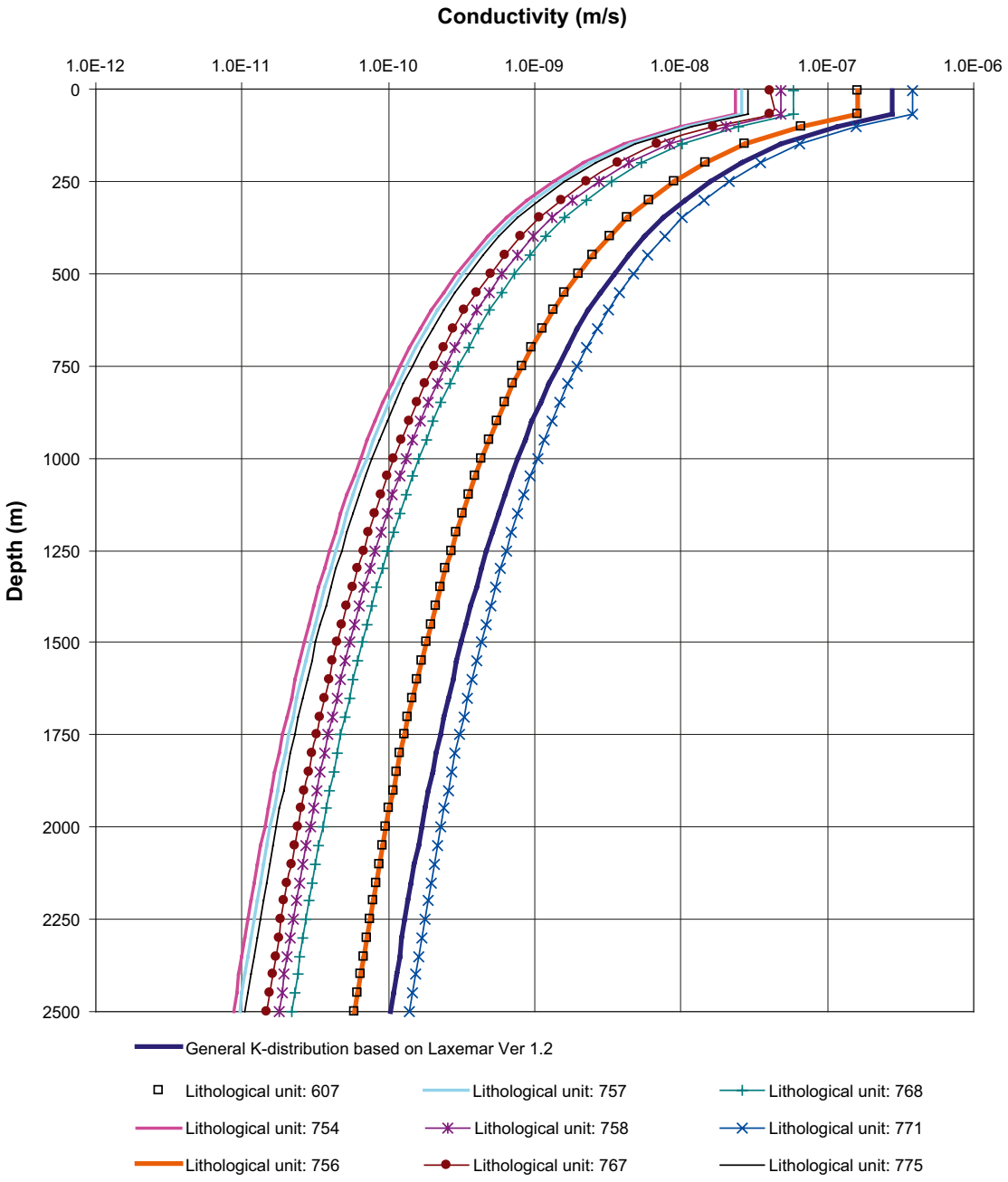

Figure 2-7. *Depth dependency of the hydraulic conductivity of the different lithological units of the rock mass. General formulation.*

2.8.2 Alternative formulation for depth dependency

An alternative formulation of the depth dependency has been used for alternative Case 1; the alternative formulation is presented below. For the base case (presented in the previous section), the depth dependency follows a smooth curve as defined in /Rhén et al. 2006/ (Laxemar site description version 1.2). However, in the flow modelling by /Hartley et al. 2006/ (SKB R-06-23 – Laxemar site description version 1.2) a step function was used instead of the smooth curve. The step function applied was adjusted to the smooth curve in a way that a good match was achieved between the two methods of describing the depth dependency, considering depths above approximately 1,500 m. A comparison of the two formulations is given below in Figure 2-8.

For the alternative case the different smooth functions that represent the lithological units and deformation zones are replaced by different step-functions. The step-functions were adjusted to match the different curves that represented the lithological units and the deformation zones of the general formulation, in the same way as in Figure 2-8.

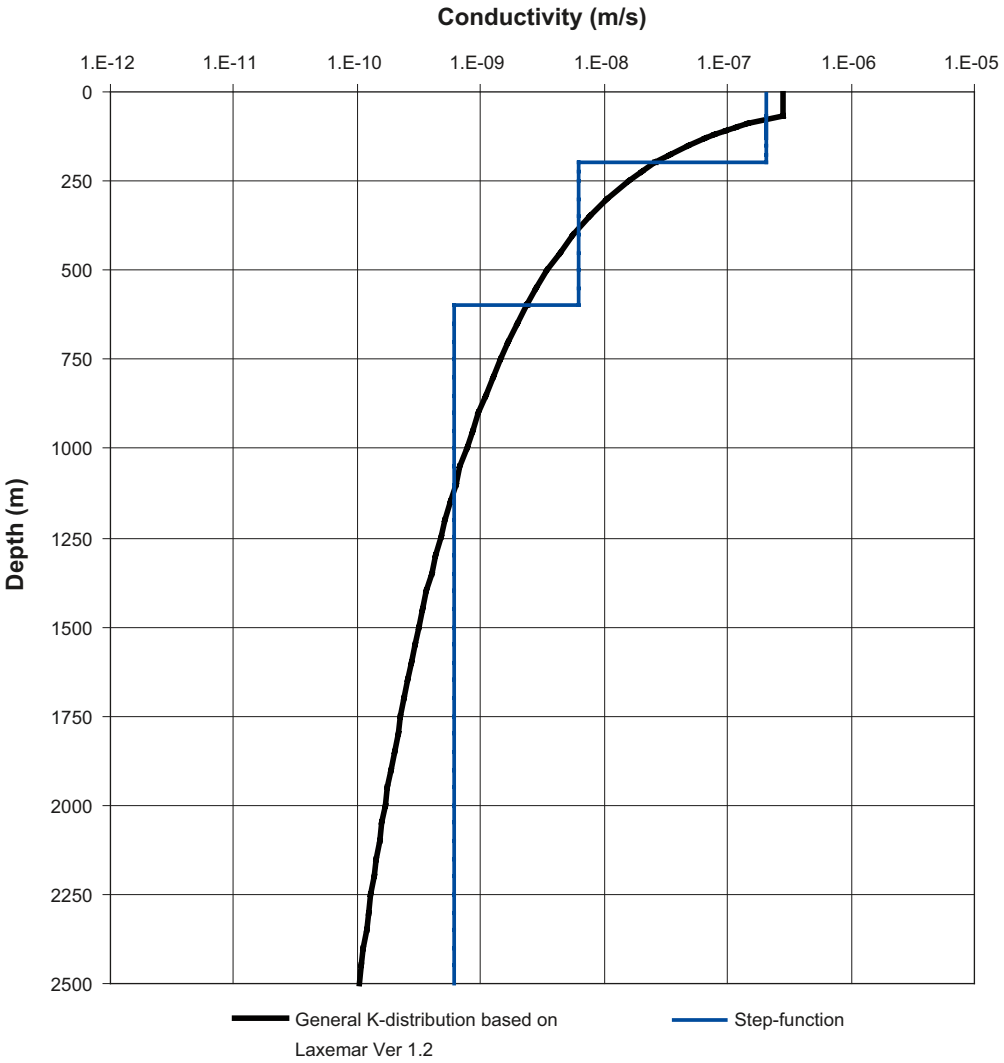

Figure 2-8. *Depth dependency of the hydraulic conductivity of the different lithological units of the rock mass. General formulation and alternative step-function.*

2.7 Fracture zones

The model includes supraregional fracture zones as well as regional and local fracture zones. The supraregional fracture zones were taken from the supraregional modelling, see /Ericsson et al. 2006/. The regional and local fracture zones were taken from the site descriptive modelling version 1.2, as defined in R-06-22 /Rhén et al. 2006/.

The extension of the supraregional fracture zones are primarily based on data provided by SGU, as well as on results from the site investigations carried out by SKB, this is discussed in /Ericsson et al. 2006/. All supraregional fracture zones are defined as vertical and they extend down do the base of the model (–2,500 m above sea level).

The supraregional zones populate the domain outside of the regional investigation area, inside the regional investigation area the model includes regional and local fracture zones. At the boundary of the regional investigation area the supraregional zones were truncated and as much as possible connected to corresponding regional fracture zones.

The supraregional fracture zones are presented in Figure 2-9, the local and regional fracture zones are presented in Figure 2-10.

Each fracture zone is defined as an explicit structure in the computational grid; hence a cell representing a fracture zone represents the fracture zone only and no part of the surrounding rock mass. The local and regional zones were defined with a hydraulic width of 50 m, the supraregional zones were defined with a hydraulic width of 100 m.

The values of hydraulic conductivity of the fracture zones are defined as depth dependent, and the depth dependency is based on the site investigations /see Rhén et al. 2006/. A power law relationship is proposed in that study, as well as an exponential relationship, we have chosen to use the power law relationship:

$T = C \cdot z^L$

Were: $C = 0.219$ and $L = -1.783$

The depth trend is given by the exponent L. The coefficient C defines properties for an average fracture zone.

Supraregional fracture zones

The supraregional fracture zones are defined as representing an average fracture zone. The same definition was used in the supraregional modelling /Ericsson et al. 2006/. As for the lithological units, the K-values above a depth of 67 m are set as constant, and below a depth of 67 m the K-values are decreasing. The following equation has been applied for the supraregional zones.

Transmissivity: $d > 67\ m \rightarrow \quad T = C\, d^L$

$d <= 67\ m \rightarrow \quad T = T_{67m}$

Conductivity: $K = T/w$

d = Depth [m]

T = Transmissivity of the fracture zone (deformation zone) [m^2/s]

T_{67m} = Transmissivity of the fracture zone at a depth of 67 m [m^2/s]

$C = 0.219$

$L = -1.783$ (trend for depth dependency)

K= Hydraulic conductivity [m/s]

w = Hydraulic width [m]

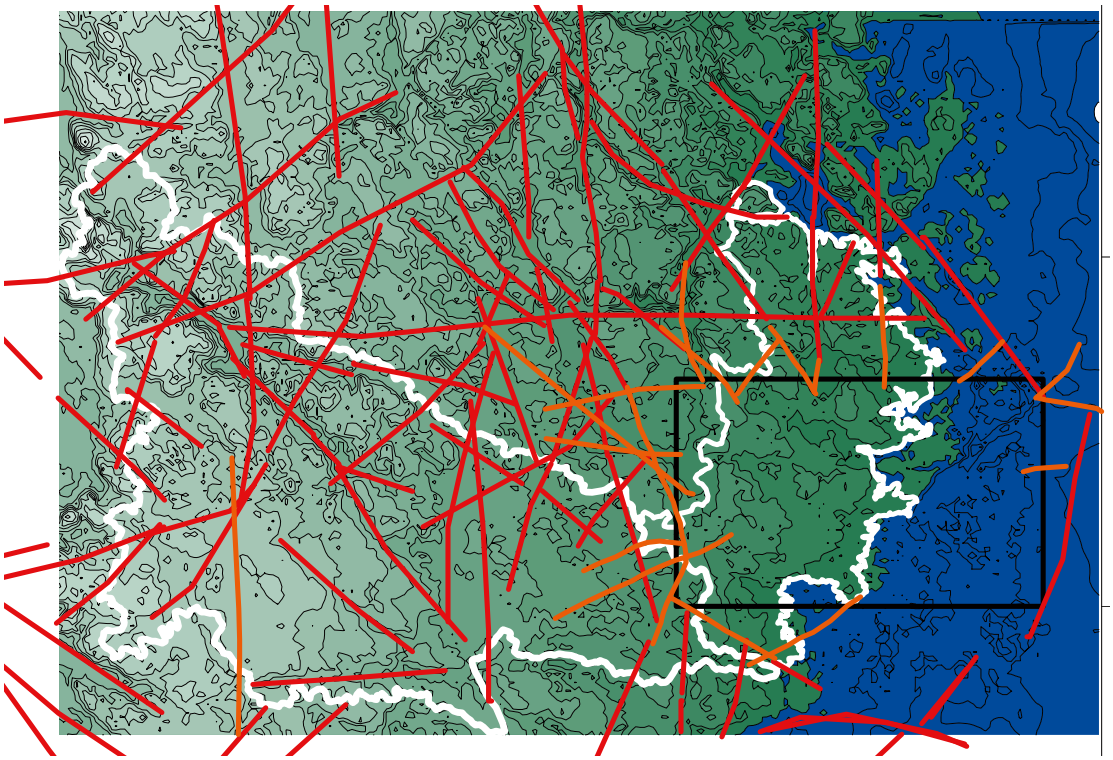

Figure 2-9. *Supraregional fracture zones as implemented in the model (red and orange lines). All supraregional zones are defined as vertical.*

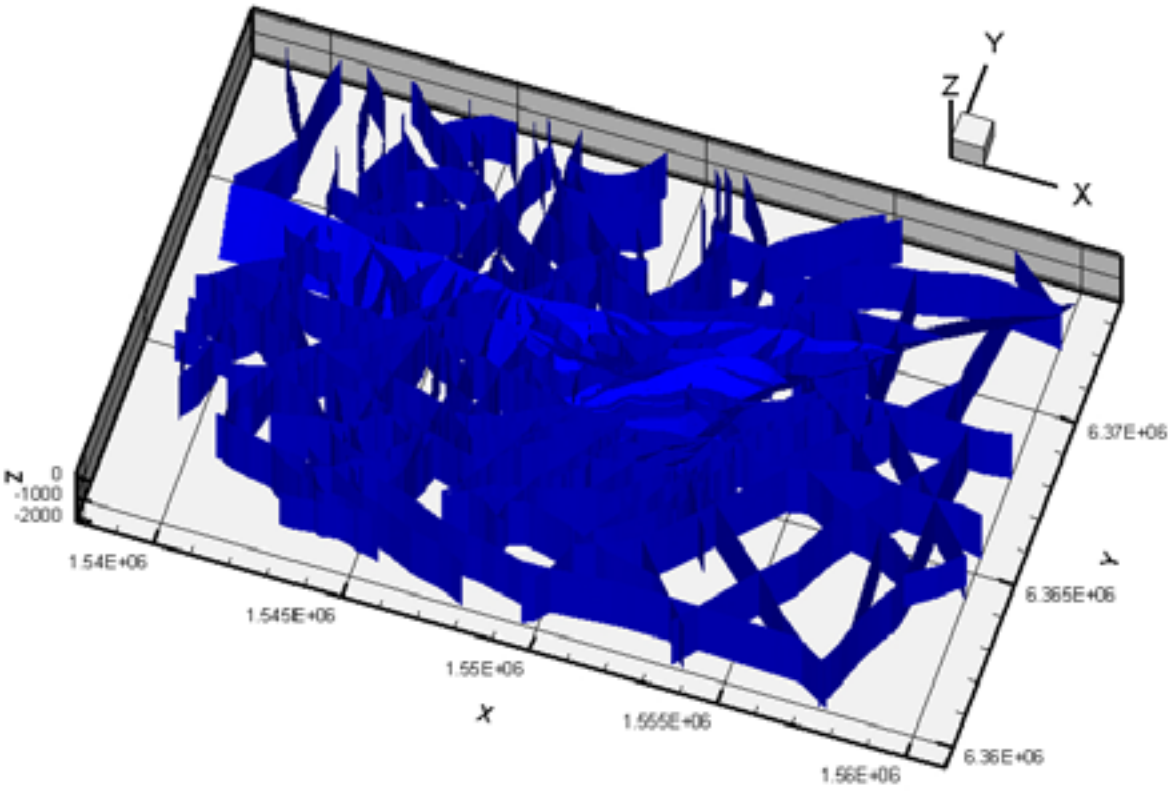

Figure 2-10. *Local and regional fracture zones as defined in the model.*

Local and regional fracture zones

The transmissivity of the local and regional fracture zones are defined in line with the values given in /Rhén et al. 2006, Table 5-2, page 29/. In this table detailed data is given for 25 fracture zones. A scale dependency has been calculated for each of these zones based on the "sample mean elevation" and the "mean Log10(T)", as given in the table. The trend for the depth dependency is based on the power law discussed above (the site investigations); the exponent is set to –1.783. For each zone a depth dependency function was calibrated in a way that the function matched the given "mean Log10(T)" at the "sample mean elevation". Above a depth of 67 m the T-values were set as constant. The following equation has been used:

Transmissivity: $d > 67\ m \rightarrow \quad T = C\ d^{L}$

$d <= 67\ m \rightarrow \quad T = T_{67m}$

Conductivity: $K = T/w$

d = Depth [m]

T = Transmissivity of the fracture zone (deformation zone) [m^2/s]

T_{67m} = Transmissivity of the fracture zone at a depth of 67 m [m^2/s]

C = A coefficient selected in a way that the calculated T-value matches the "mean Log10(T)" at the "sample mean elevation".

L = –1.783 (trend for depth dependency)

K= Hydraulic conductivity [m/s]

w = Hydraulic width [m]

As mentioned above, each fracture zone is defined as an explicit structure in the computational grid; hence a cell representing a fracture zone represents the fracture zone only and no part of the surrounding rock mass. The K-values of the zones were defined for a hydraulic width of 50 m. For a few of the zones given in R-06-22, Table 5-2 (ZSMEW014A, ZSMEW013A, ZSMNE015A, ZSMNE016A, ZSMNW025A), the obtained K-values for a hydraulic width of 50 m are smaller than or very similar to the average K-values of the surrounding rock-mass. This follows from the actual widths of these zones, which are probably much less than 50 m. In the model these fracture zones are assigned K-values in line with the surrounding rock mass; the zones will however be distinguished by the cells sizes, which are smaller for the zones than for the surrounding rock mass.

The structural geological model of the regional and local fracture zones contains more than 170 different fracture zones. Detailed transmissivity data is only given for 25 zones in R-06-22 – Table 5-2, all other fracture zones have been assigned average properties, as for the supraregional zones (C = 0.219 and L = –1.783).

The rock mass of the lithological units are defined as heterogeneous by use of a stochastic continuum approach. The methodology for the stochastic continuum approach is discussed in Appendix A.

Examples of the calculated (calibrated) depth dependencies of different fracture zones are given in Figure 2-11.

Local and regional fracture zones – alternative formulation of depth dependency

As previously discussed in Section 2.6.2, we have analysed an alternative formulation of the depth dependency of the hydraulic conductivity. The step-function discussed in Section 2.6.2 has also been used for the deformation zones of the alternative Case 1 (see also Section 2.6.2).

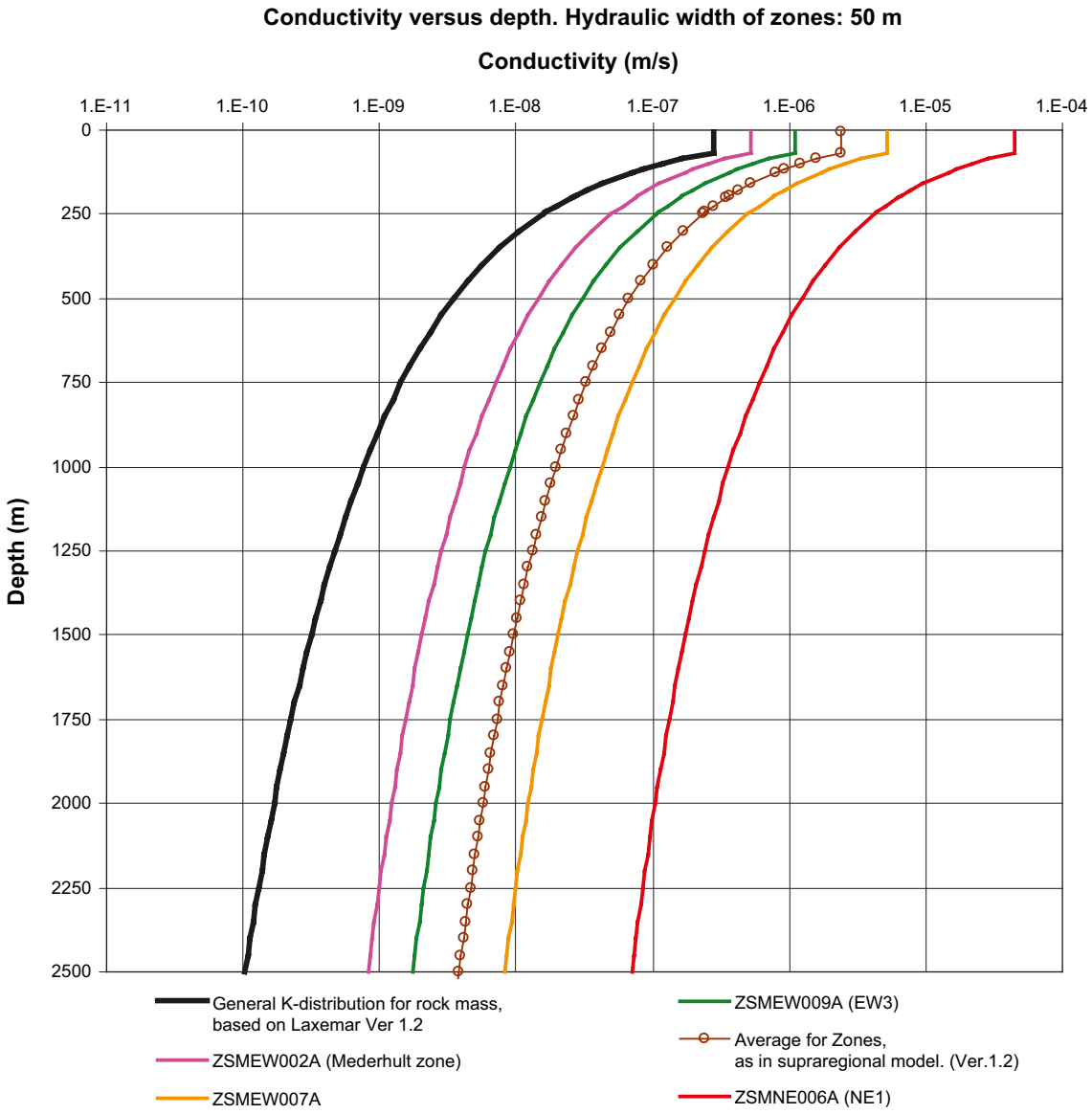

Figure 2-11. *Depth dependency for fracture zones as implemented din the model. Examples of the calculated depth dependencies of different fracture zones.*

2.8 Quaternary deposits

Quaternary deposits occur on top of the model. The extensions and depths of these deposits are based on data provided by SGU (Swedish Geological Survey), see /Ericsson et al. 2006/. The area is dominated by glacial till (morain) with a depth of 1 m to 3 m, close to the shore line the depths of the till is less than 1 m. Glaciofluvial deposits occur in elongated structures i.e. eskers, directed in an approximate NW-SE direction. The quaternary deposits – as implemented in the model – are given below in Figure 2-12.

The values of hydraulic conductivity of the quaternary deposits are the same as in /Ericsson et al. 2006/.

- Glacifluvial deposits K = 1E–4 m/s
- Glacial till (morain) K = 1E–6 m/s

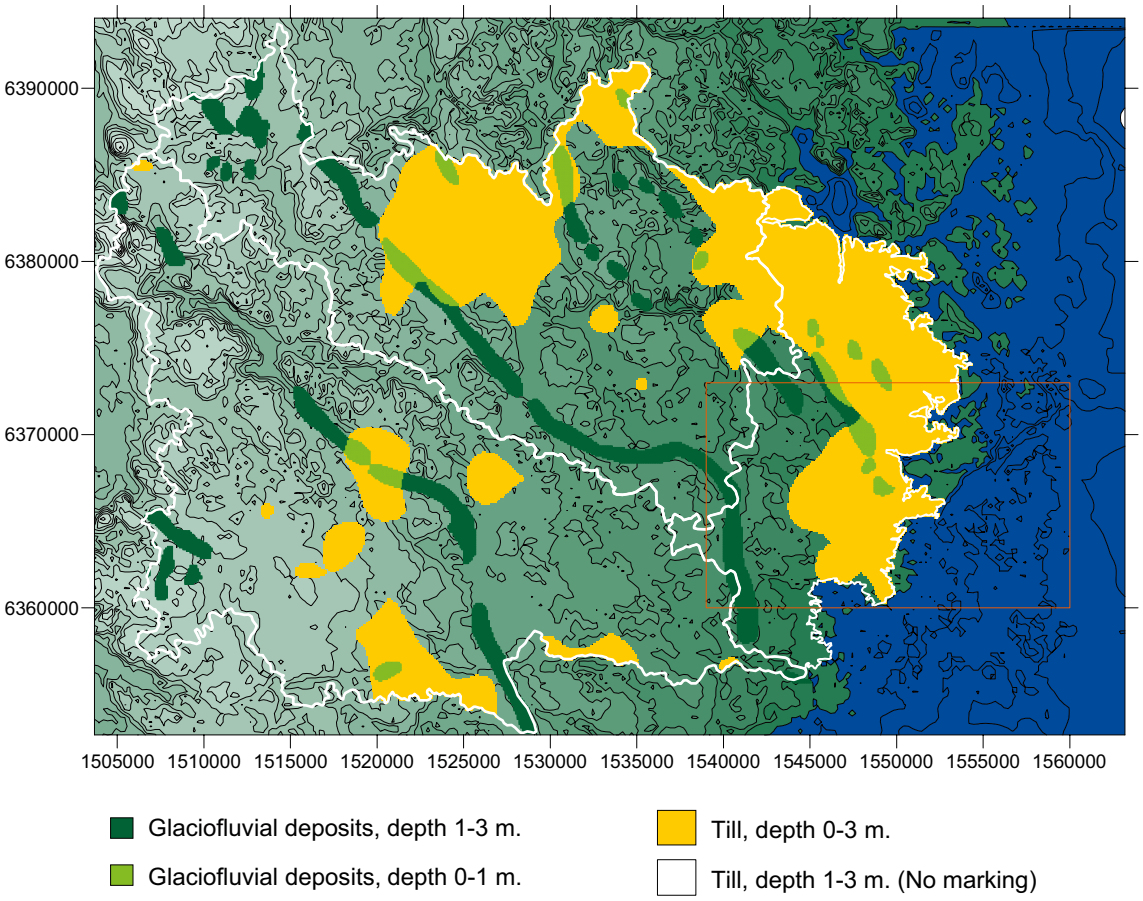

Figure 2-12. *Quaternary deposits as defined in model.*

In the established models, for numerical reasons, the quaternary deposits have been scaled to a constant thickness of 10 m; the conductivity values of the different deposits have been scaled in accordance, see /Ericsson et al. 2006/.

2.9 Porosity and transport resistance

The effective porosity (kinetic porosity or transport porosity) is defined as the ratio of the volume of interconnected pore-space (or fracture-space) available for fluid transmission to bulk volume of the soil or the rock. The calculated advective breakthrough times are directly proportional to the effective porosity.

In the established model the effective porosity is set to **0.001** for all geological units and structures.

The models have been assigned this constant value of porosity because it is a value that has been used in previous studies /Voss and Provost 2001, Follin and Svensson 2003, Holmén et al. 2003, Ericsson et al. 2006/ which facilitates a comparison between the result of this study and the previous studies, and also because it is reasonable integrated value for the rock masses (see for example /Carlsson and Gustafsson 1984/. There is however an additional reason which is discussed below.

In comparison to the advective flow of groundwater, components dissolved in the groundwater will be delayed due to different retention processes, e.g. sorption and matrix diffusion. Matrix diffusion is the process at which a dissolved component diffuses from the moving water in fractures (and pores) into the stagnant water of the rock-matrix. Matrix diffusion is a very

important retention process and the delay of the transport of dissolved components that takes place because of matrix diffusion is described by a parameter called the transport resistance parameter, or F.

In a simplified way the transport resistance can be described as the surface area of a flow route (channel) divided with the groundwater flow along the flow route. Considering a flow route with constant geometry, the transport resistance can be written as follows:

$$F = a_r \frac{L}{q} \qquad \text{Equation 2-1}$$

F = Transport resistance (Time/Length)

a_r = Flow wetted surface area per volume of rock (Length^2/Length^3 = 1/Length)

L = Length of flow route (Length)

q = Specific flow or the darcy velocity (Length/Time)

If the geometry varies along the flow route, the formulation of the transport resistance will be more complicated, this is discussed in the EU project /EU RETROCK 2005/.

The quota L/q in the equation above can be calculated by use of a groundwater model for different sections along the flow route (e.g. from starting point to the discharge area); and the obtained values of the quota can be added together to a total value, presuming that a_r parameter is constant along the flow route.

In addition, if the porosity is approximated by a constant value along the flow route, the quota (L/q) can easily be calculated based on the advective break-through times, in the following way:

$$\sum \frac{L}{q} = \frac{1}{\eta} t_{breakthrough} \qquad \text{Equation 2-2}$$

η = Effective porosity (–)

$t_{reakthrough}$ = Calculated advective breakthrough time (Time)

By combining the two equations above (Equation 2-1 and Equation 2-2) the following equation will be obtained:

$$F = a_r \frac{1}{\eta} t_{breakthroug} \qquad \text{Equation 2-3}$$

From Equation 2-3 we conclude that the transport resistance will be directly proportional to the breakthrough time if the following two parameters are defined as constant along the flow route: (i) the effective porosity and (ii) the flow wetted surface area per volume of rock.

This is one of the reasons why we have used a constant porosity in this study. By using a constant porosity in the established models the transport resistance will be proportional to the breakthrough time (even if the absolute values are not the same) and for the model a comparison of different breakthrough times is also a comparison of the transport resistances.

2.10 Boundary conditions and initial condition

The model is defined with the no-flow boundary condition along the base of the model and along the lateral boundaries of the model. The lateral boundaries follows regional surface water divides that we assume can be approximated as groundwater divides.

Along the top of the model the specified pressure condition is applied. Above the shore-line the specified pressure condition simulates approximately a groundwater surface that follows the topography. This is a reasonable condition, because of the large values of precipitation and run-off that occur at the area studied; this is discussed in more detail in /Ericsson et al. 2006/.

The groundwater surface is defined along the undulating topography above the sea, except at Glaciofluvial deposits (eskers). Inside the highly transmissive eskers the groundwater surface is not defined along the topography of the eskers, but along interpolated surfaces with elevations given by the topography of the surrounding materials. By use of this approach the model will approximately reproduce the elevation of the groundwater surface inside the eskers.

Below the sea the specified pressure is defined along the sea floor. At the sea floor the specified pressure is given by the salinity of the sea water and the depth of the sea.

The case studied is a time dependent case that simulates the shore-level progress and density dependent flow. The starting time is set to 10,000 years before present. The model includes therefore also boundary conditions for the distribution of salinity. At the base of the model a specified salinity is defined, equal to 10%. A salinity of 10% corresponds to 100 grams of total dissolved solids (TDS) per litre of water, which is approximately equal to 0.1 Kg TDS/Kg. Along the upper surface of the model, above the moving shoreline, fresh water will infiltrate into the model. Finally the salinity of the sea will vary with simulation time, reproducing the different stages of the Baltic Sea.

A schematic presentation of the boundary conditions of the model is given in Figure 2-13.

In the model the shore line will move during the transient simulation from the elevation at the initial condition 10,000 years before present (10,000 years BP) to the present elevation, this procedure simulates the land rise (land upheaval) and the different stages of the Baltic sea (see also /Ericsson et al. 2006/. The applied movement of the shoreline is given in Figure 2-14. The position of the sea at the initial condition is given in Figure 2-15.

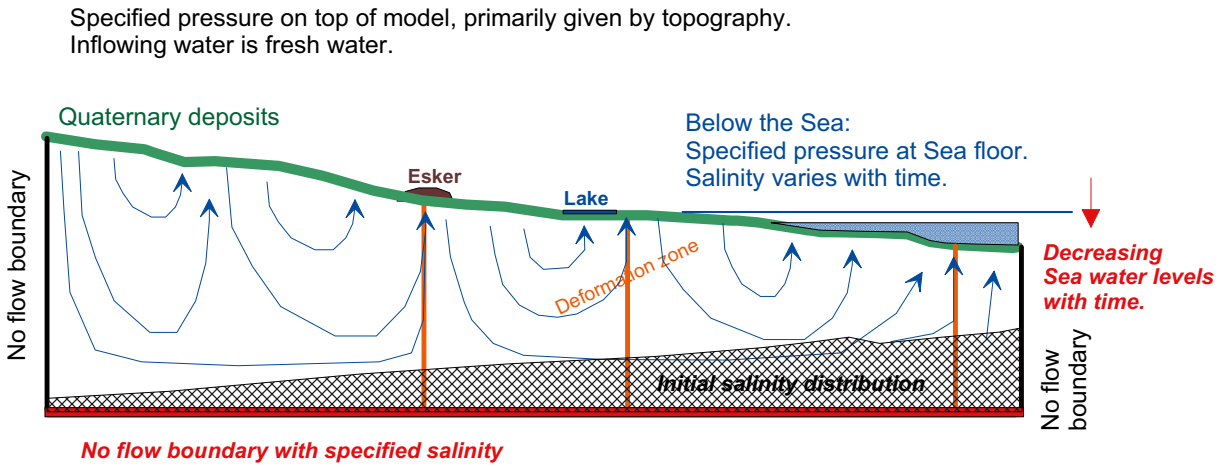

Figure 2-13. *Schematic presentation of the boundary conditions of the model.*

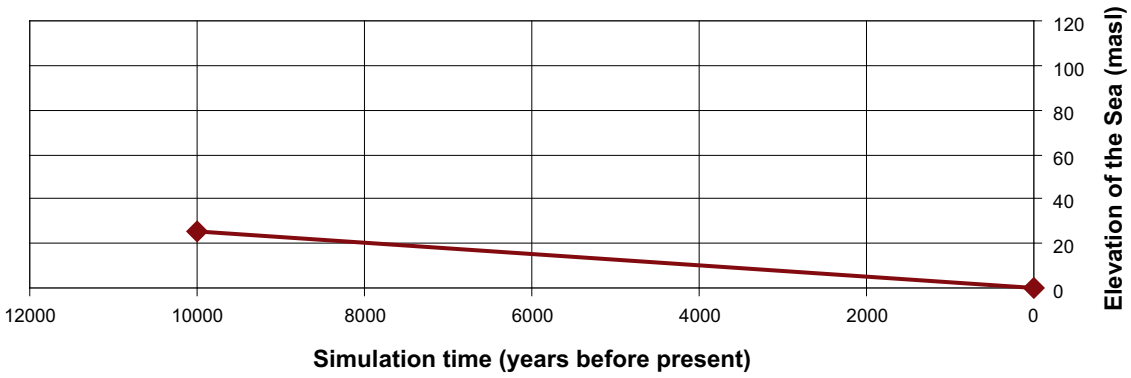

Figure 2-14. *Elevation of the sea versus simulation time.*

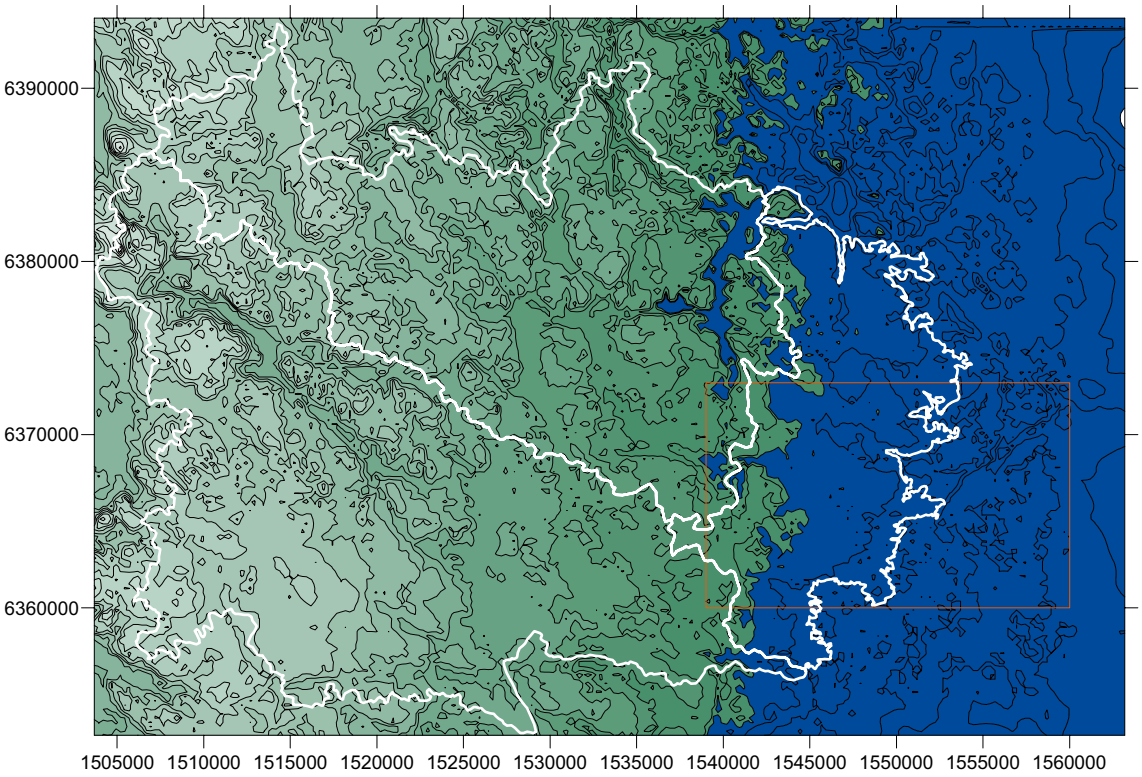

Figure 2-15. *Position of the sea at the initial condition, 10,000 years BP. The sea is at an elevation of +25 m above sea level.*

In the model the salinity of the sea will also change with time, reproducing the different stages of the Baltic Sea /see also Ericsson et al. 2006/. The Salinity versus simulation time is given in Figure 2-16.

The model is also assigned an initial condition considering the salinity distribution. The applied initial condition is the same as condition **s2** in /Ericsson et al. 2006/. The elevation of the saline water is related to the topography, in a way that lower elevations of the saline water will occur for high elevations of the topography. The following relationship has been applied:

- If the topography is < = +100 m above sea level, the saline water will start at en elevation of Z = –700 m above sea level.
- If the topography is > +100 m above sea level, the saline water will start at en elevation given by the following equation: Z = –5.385 * Topo – 161.54.

Above the Z-level the salinity is set to zero, below the Z-level and down to the base of the model (–2,500 m above sea level) the salinity will increase in a linear way from zero to 10%

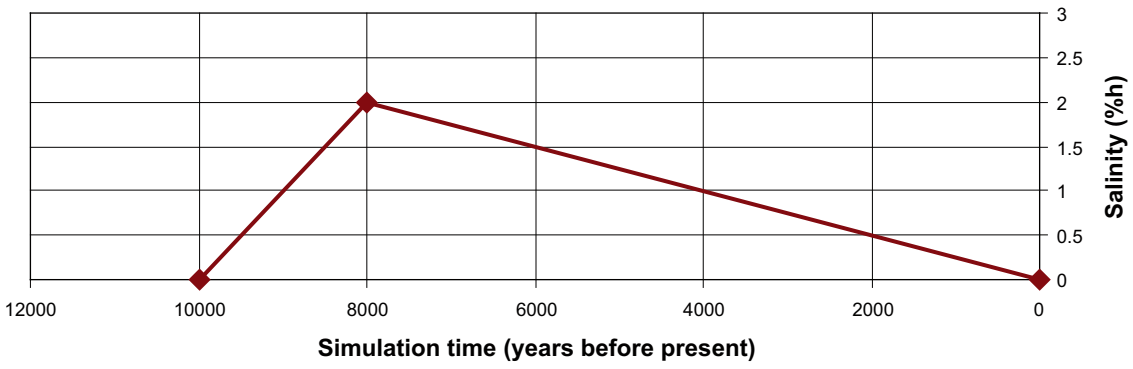

Figure 2-16. *Salinity of the sea versus simulation time.*

(the salinity at the base of the model is 10%). This initial condition is presented in Figure 2-17. Figure 2-17 demonstrates that the initial distribution of salinity is not much influenced by the undulation of the topography; this is because the topography is below +100 m above sea level for most of the presented cross-section (see the equation above).

The relationship presented above between topography and salinity should only be looked upon as an approximate method for deriving a reasonable initial condition. The condition is partly based on the highest elevation of the Baltic Sea at the area studied, considering the different stages of the Baltic Sea since the last glacial period; which corresponds to an elevation of approximately +100 m above sea level.

2.11 The computational grid

The model consists of a very large number of three-dimensional cells, assembled in a system of columns rows and layers, together forming the computational grid. The models have been established by use of the DarcyTools 3.0 computer code (DT30). The DT30 code uses an unstructured grid, which means that the number of columns, rows and layers may vary inside the model.

In DT30 the computational grid is created by use of three-dimensional objects that represents different geological structures of the domain studied, e.g. lithological units and fracture zones, as well as the surface defining the topography. The resolution of the grid is defined for each object separately.

The following cell sizes have been used:

- At ground surface, largest cells: Lx, Ly, Lz [m]: 50×50×3.
- Quaternary deposits below ground surface, largest cells Lx, Ly, Lz [m]: 100×100×4.

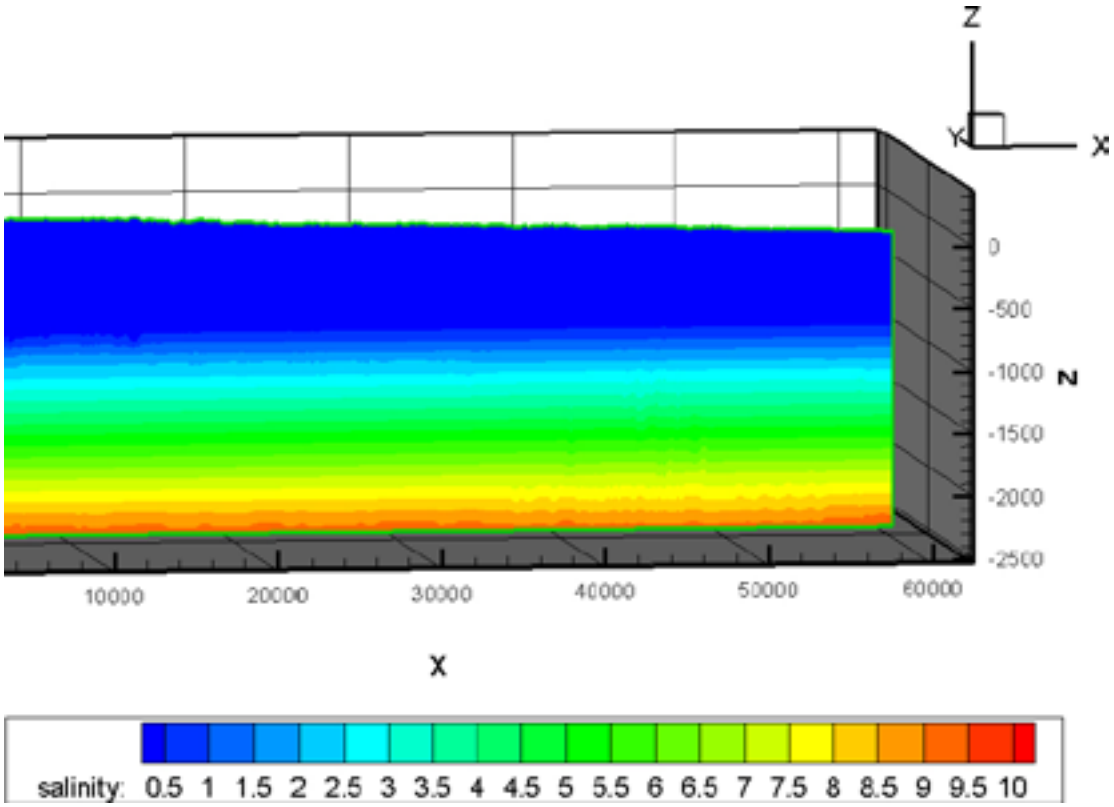

Figure 2-17. *The initial distribution of salinity. A salinity of 10% corresponds to 100 grams of total dissolved solids (TDS) per litre of water, which is approximately equal to 0.1 Kg TDS/Kg.*

Local and regional deformation zones:

- Above a depth of 1,000 m : Lx, Ly, Lz [m]: 50×50×50.
- Below a depth of 1,000 m : Lx, Ly, Lz [m]: 50×50×200.

Supraregional deformation zones:

- Above a depth of 1,000 m : Lx, Ly, Lz [m]: 100×100×100.
- Below a depth of 1,000 m : Lx, Ly, Lz [m]: 100×100×200.
- Lithological units, largest cells: Lx, Ly, Lz [m]: 400×400×200.

The total numbers of cells are:

(i) For the large model ca. 5 millions, and,

(ii) For the small model ca. 2.2 millions.

A detailed view of the unstructured computational grid and the different cell sizes are given in Figure 2-18. As previously discussed each fracture zone is defined as an explicit structure in the computational grid. This is well demonstrated in Figure 2-18; the fracture zones are clearly visible as elongated structures defined by small cells.

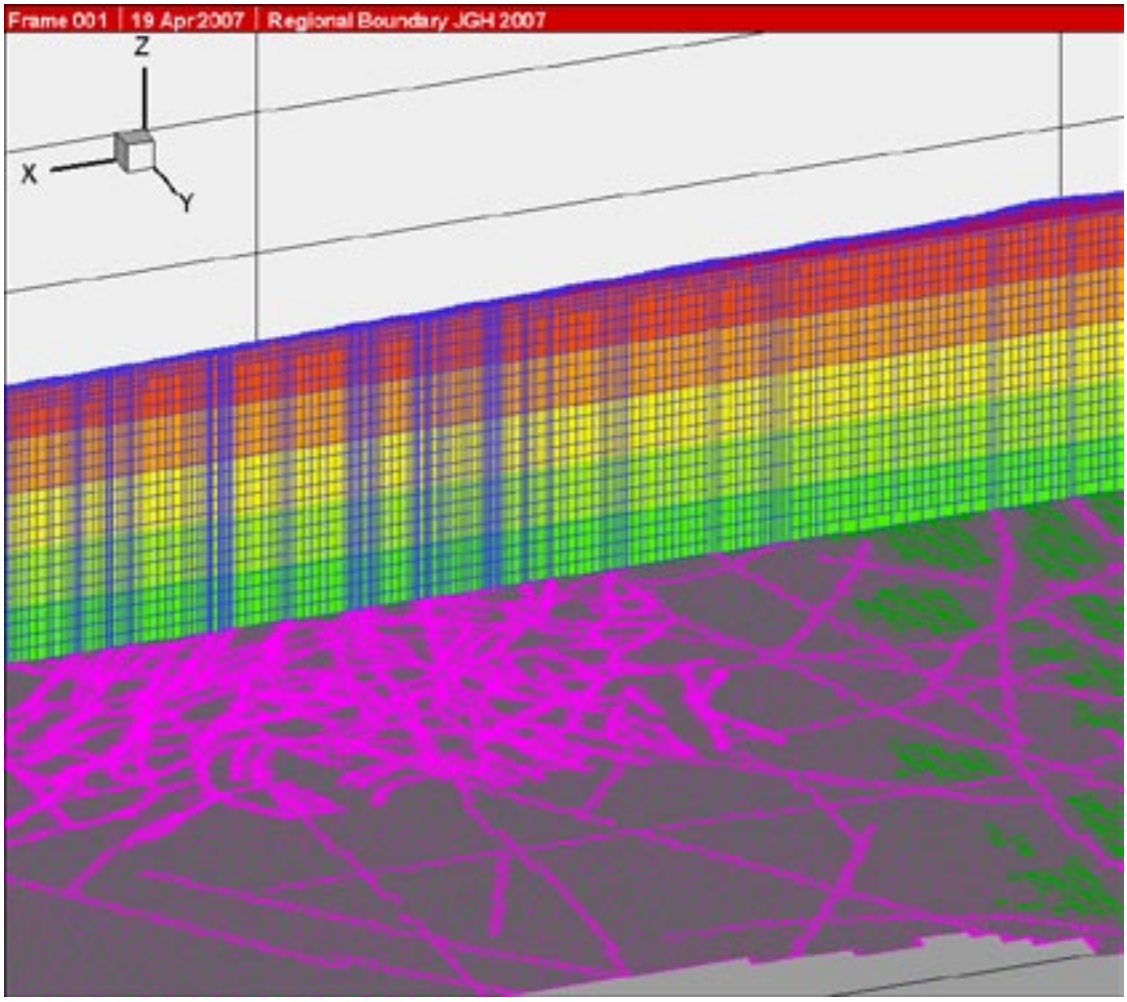

Figure 2-18. *A detailed view of the different cell sizes of the computational grid. A vertical cross-section and a horizontal cross-section. The elongated structures with small cells are the fracture zones. The large cells to the right are the cells below a depth of 1,000 m above sea level.*

The difference between the large and the small model is that the part of the grid that is located west of the studied topographic surface water divide (see Figure 2-3 and Figure 2-4) is set as inactive in the small model. Hence, inside the domain that takes place in both models, the grid is exactly the same.

A comparison of the grid of the large and small models is given by Figure 2-19 and Figure 2-20.

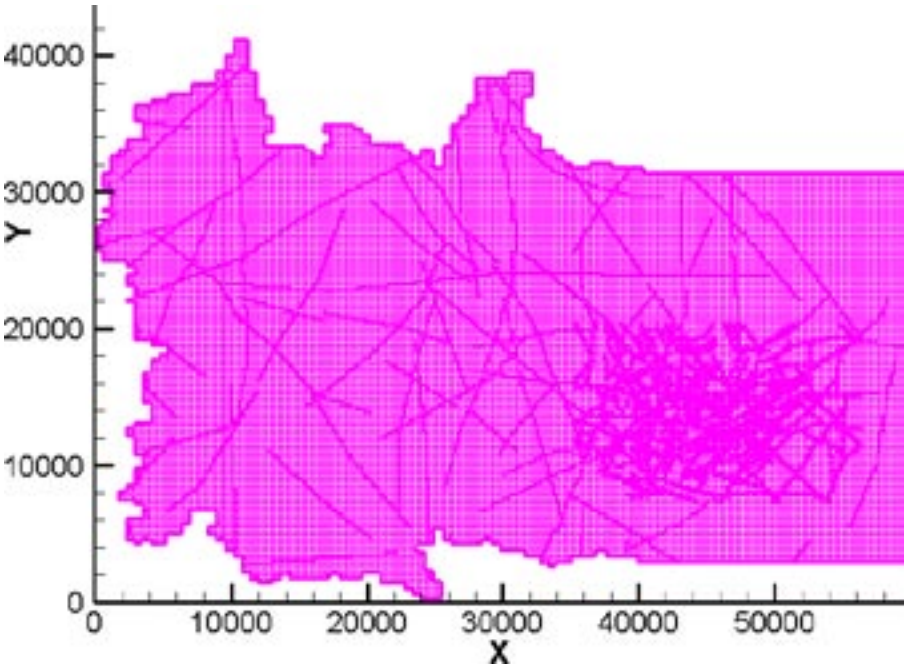

Figure 2-19. *Grid of large model at a depth of 500 m.*

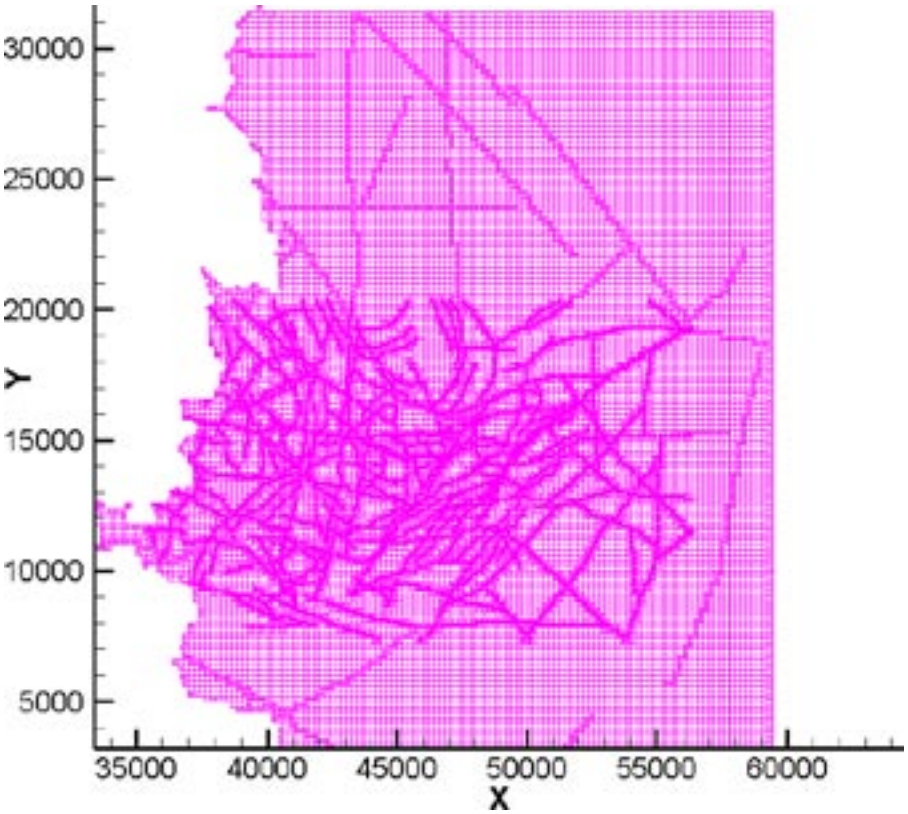

Figure 2-20. *Grid of small model at a depth of 500 m.*

3 Horizontal size of grid cells and representation of water divides

3.1 Introduction and objectives

The local and regional topographic undulation is of importance for the groundwater flow pattern; this is discussed in /Ericsson et al. 2006/. Therefore topographic surface water divides may be used as approximate no-flow boundaries in groundwater models.

The studied topographic surface water divide between (i) Basin 3 and (ii) Basins 1 and 2 (see Figure 2-3f and Figure 2-4) is defined as a no-flow boundary (i.e. as a groundwater divide) in the regional flow modelling of the site investigations (see Figure 2-5).

Both west and east of the above discussed weakly developed surface water divide, the topography is gently dipping towards the sea (on a regional scale). The surface water divide is "weakly developed" as it is only a consistent surface water divide if the topography is analysed with a very fine resolution. If the topography is analysed with a resolution of e.g. 100 m (or larger), it is likely that the regional topographic gradient (gently dipping towards the sea) will come to dominate the analysis and the weakly developed surface water divide will not show up as a consistent surface water divide in such an analysis.

If this weakly developed topographic ridge is to act as a surface water divide, and as an important element of a groundwater flow model, it needs to be defined with a high resolution in a groundwater model. The number of cells in a groundwater model needs however to be limited due to numerical reasons.

The objective of this chapter is to find the necessary geometric resolution (i.e. horizontal size) of the computational cells along the topography of a groundwater model, for the purpose of correctly representing the above discussed topographic surface water divides.

3.2 Methodology and computer code

The analyses were based on simulated surface water flow paths. The analyses were carried out by use of the surface water routines of the GEOAN computer code /Holmén 1997/. The surface water flow paths were generated upstream from Basin 3 (the drainage basins are presented in Figure 2-3). The simulated surface water flow paths follow the topographic gradient upstream until a surface water divide is found. Hence, the studied surface water flow paths do not follow the topographic gradient downstream, but upstream to the top of any topographic maxima (where they will stop). The analyses were carried out without any actual flow calculations. The analyses considered the geometry only of the upper surface of different models with different cell sizes. The upper surface of the models should represent the topography.

The topographic elevations given to the cells of the different models were based on interpolation from the topographic elevations as given in the topographic data-base. As discussed in Section 2.4, the supraregional topography is given by the national grid ("Rikets nät") with a resolution of 50×50 m. At the regional investigation area, and somewhat outside of this area, the data from the national grid were replaced by local topographic data: The resolution of the local topographic data varies between 50×50 m and down to a resolution of 20×20 m (see Figure 3-1).

The interpolation was based on the method "weighted inverse distance"; the weighting power was set to 3. For cells having a horizontal size > = ca. 50×50 m, there will be several topographic data-values within each cell.

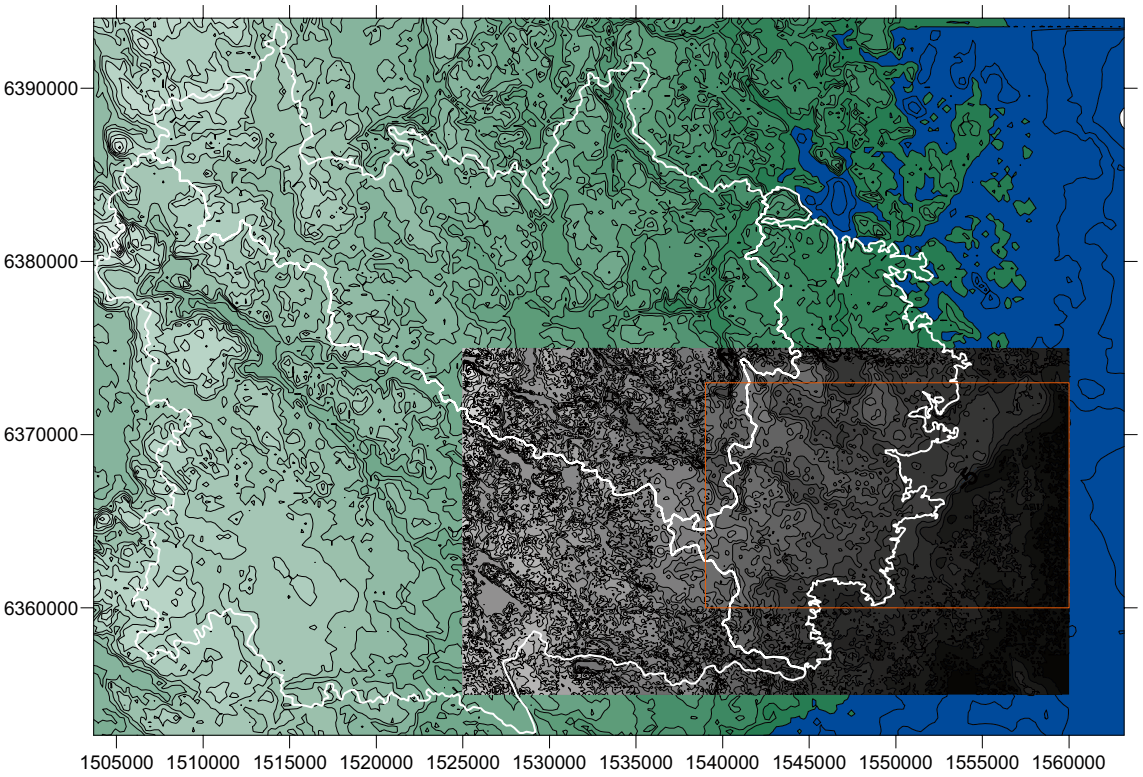

Figure 3-1. *The different domains with topographic data: For the green area the topography was based on the national grid with a resolution of 50×50 m. The black area represents the domain with local topographic data, for some parts of this domain the data-resolution is 20×20 m.*

Four different models were established with different horizontal cell sizes along the topography:

- 400×400 m
- 200×200 m
- 100×100 m
- 50×50 m

For each model 400,000 surface water flow paths were released inside Basin 3 (see Figure 3-2), these flow paths were set to move upstream along the topography.

If the models represent the surface water divides in a correct way, no upstream moving surface water flow paths from Basin 3 should penetrate into Basins 1 and 2.

3.3 Results

The results of the simulations are calculated surface water drainage basins, considering upstream moving surface water flow paths released inside Basin 3. If the analysed models represent the studied surface water divides in a correct way, the calculated drainage basin should be equal to Basin 3.

Results are given in the following figures:

- For the model with a horizontal resolution of 400×400 m, see Figure 3-3.
- For the model with a horizontal resolution of 200×200 m, see Figure 3-4.
- For the model with a horizontal resolution of 100×100 m, see Figure 3-5.
- For the model with a horizontal resolution of 50×50 m, see Figure 3-6.

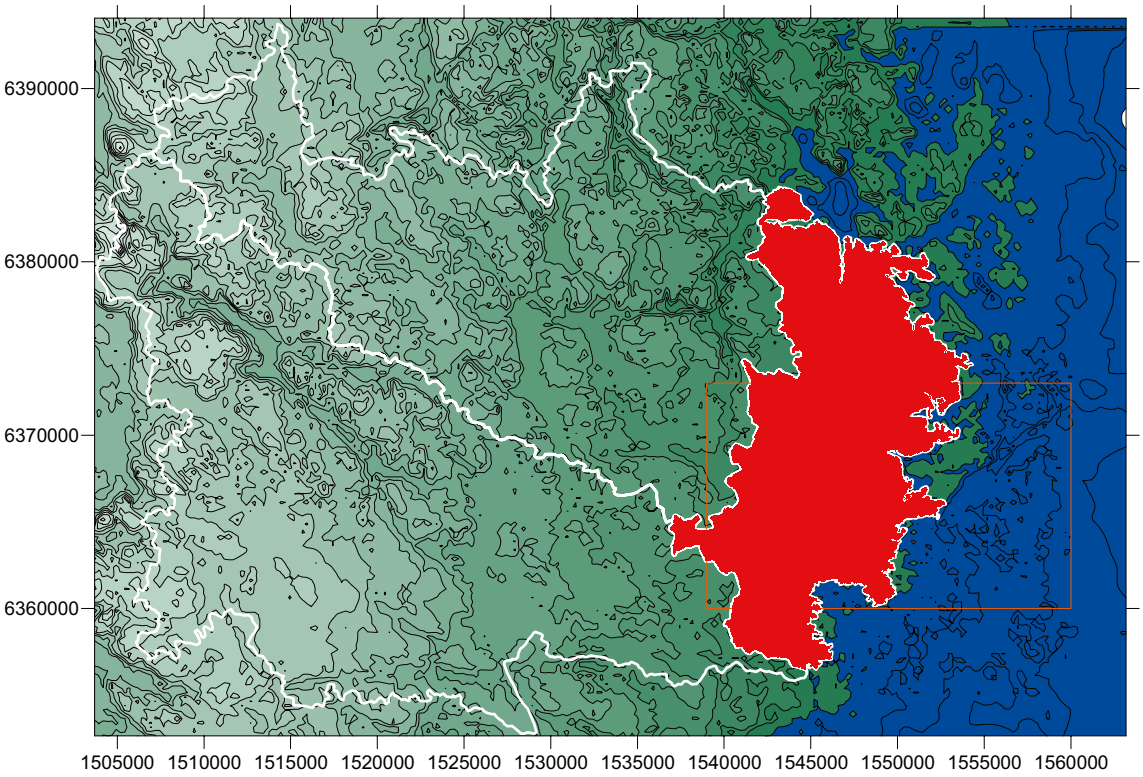

Figure 3-2. *The red area denotes the area from which the surface water flow paths were released. This area is identical to Basin 3. 400,000 flow paths were released inside this area and moved upstream along the topography.*

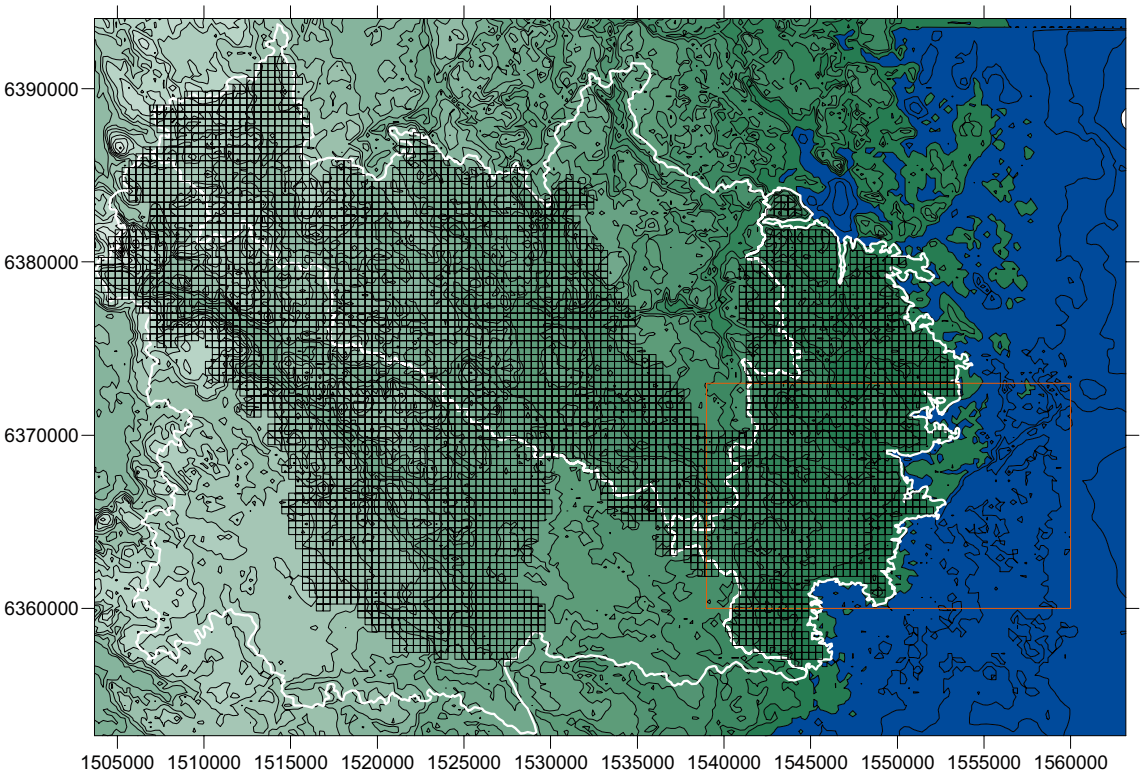

Figure 3-3. *Calculated drainage basin for surface water flow paths upstream from Basin3. Horizontal cell size is 400×400 m.*

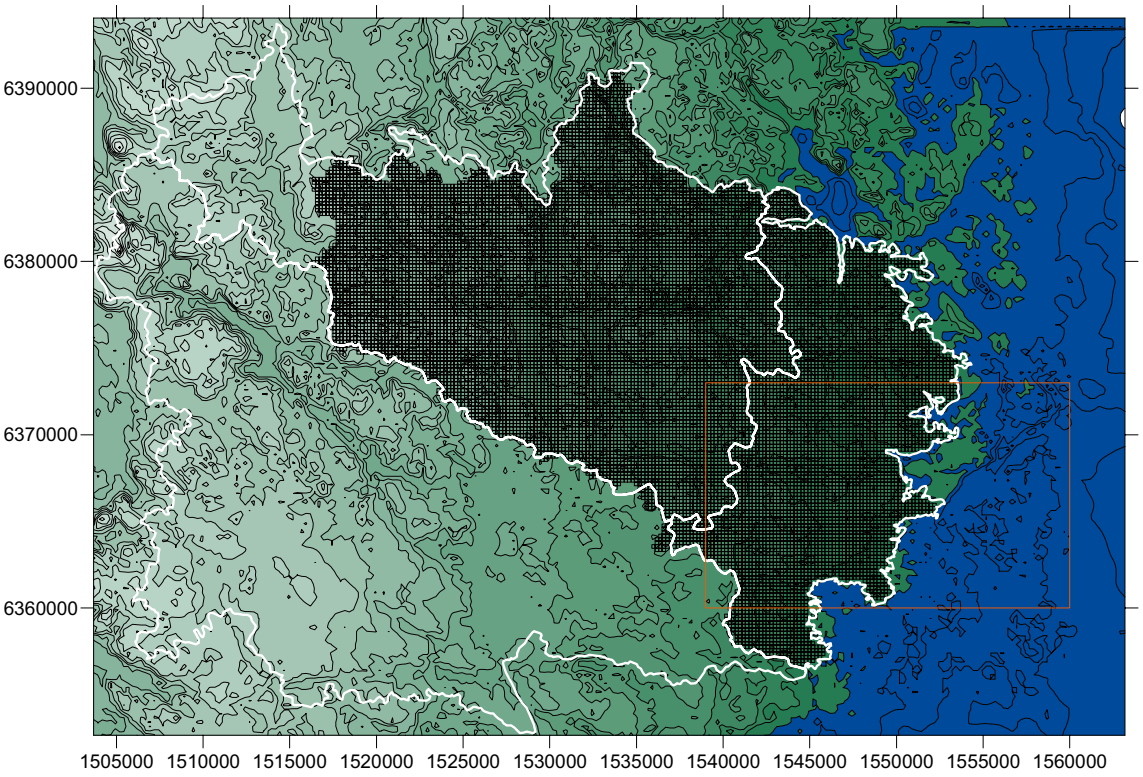

Figure 3-4. *Calculated drainage basin for surface water flow paths upstream from Basin 3. Horizontal cell size is 200×200 m.*

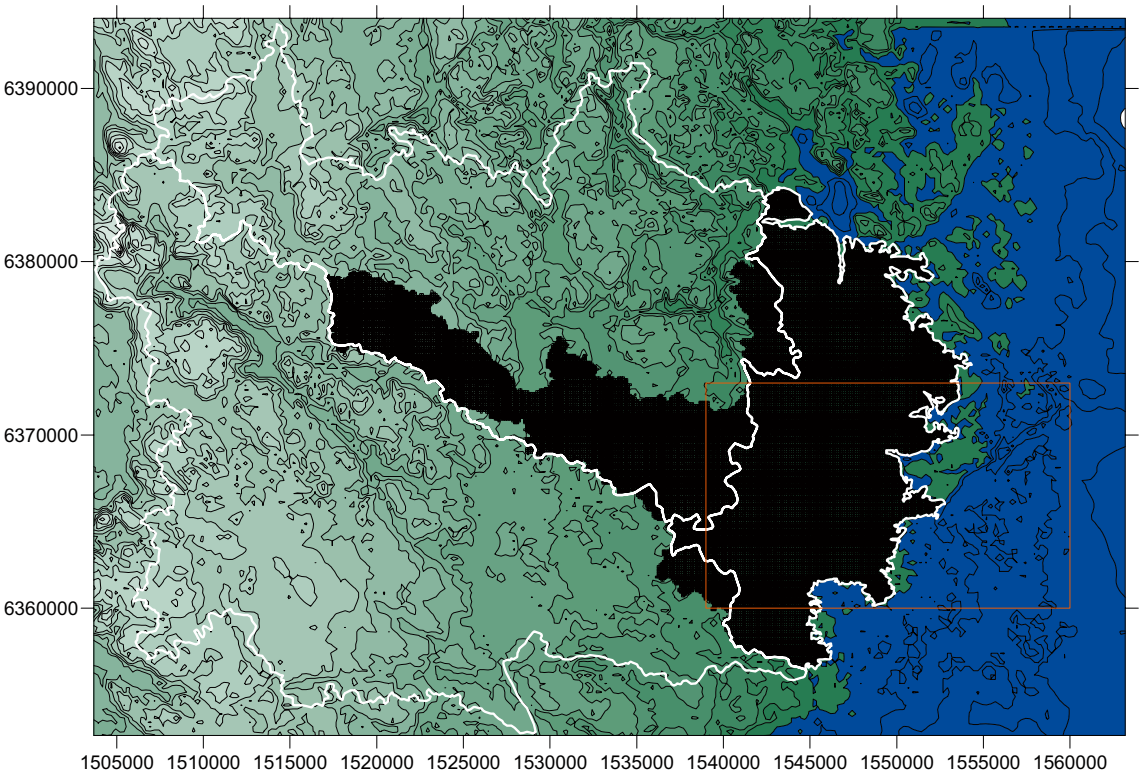

Figure 3-5. *Calculated drainage basin for surface water flow paths upstream from Basin 3. Horizontal cell size is 100×100 m.*

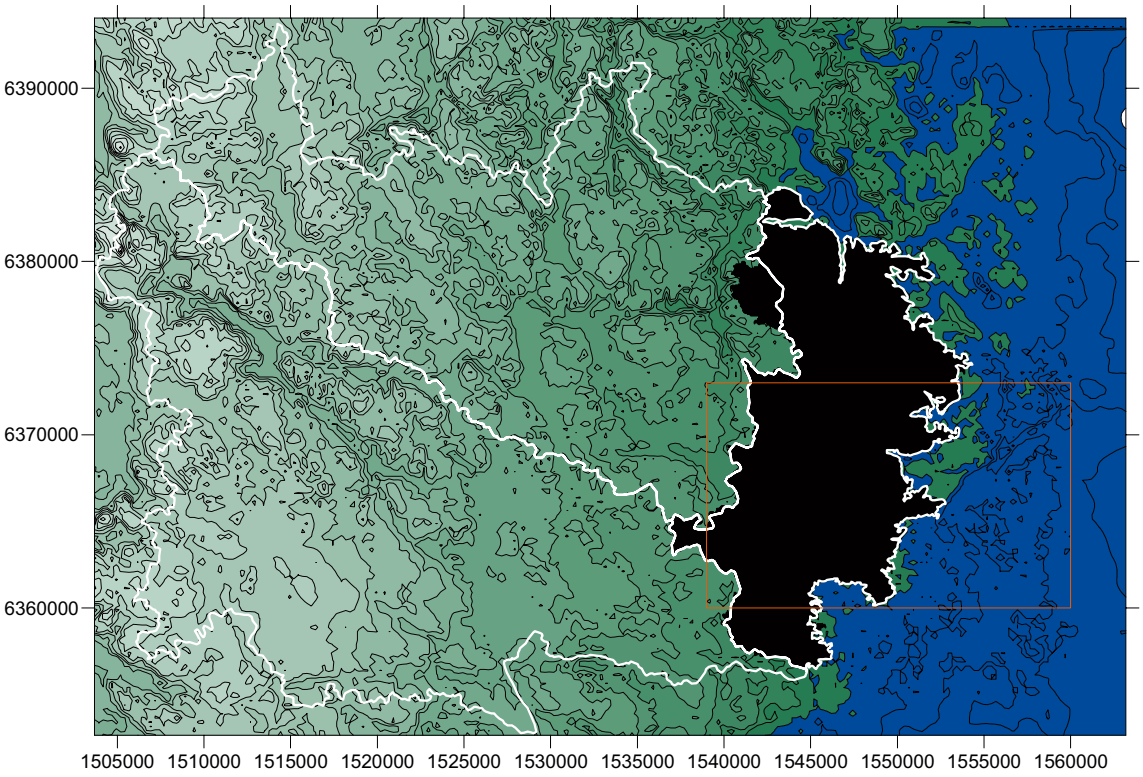

Figure 3-6. *Calculated drainage basin for surface water flow paths upstream from Basin 3. Horizontal cell size is 50×50 m.*

For the models with a resolution larger than 50×50 m, Basin 3 is not reproduced in a correct way. It is obvious that the weakly developed water divide is not represented in a correct way if the horizontal cell size is larger than ca. 50×50 m. Therefore, the horizontal cell size of the computational grid is set to 50×50 m (see Section 2.11)

It should be mentioned that the water divide can be well represented also with larger cells sizes than 50×50 m, but only by use of a more advanced interpolation routine for calculating the topographic elevation of the cells, a routine that includes additional information, like the position of the studied water divide etc.

4 Flow simulations

4.1 Introduction and objectives

The objective is to calculate and compare groundwater flow and flow paths at a tentative repository area at Laxemar; for the large flow model, and for the small flow model. The comparisons regard different aspects of the groundwater flow, and based on the comparisons we will estimates how the position of the westernmost boundary condition influences the groundwater flow at the area studied.

The comparisons include the following three parameters:

- Length of flow paths from the tentative repository area.
- Advective breakthrough time for flow paths from the tentative repository area.
- Magnitude of flow at the tentative repository area.

4.2 Methodology

The models used for simulations are described in Chapter 2. The simulations are carried out as density dependent and time dependent (transient). The simulations start with an initial condition 10,000 years before present. The simulations considers a period of 10,000 years from the initial condition and up to the present situation (2,000 AD), this is discussed in Section 2.10. Two major input-parameters change during the studied transient simulation: the position of the shore line (the shore level progress) and the salinity of the sea. The calculated flow situation at 2,000 AD is the results of the transient simulations.

The results of a time dependent simulation depend on the number of time steps and the lengths of the time steps used for representing the time dependent course. A transient simulation may include time steps of different lengths, in this study all time steps have the same length, hence the number of time steps gives the length of the time step. A time step may be divided into sub-time steps, the sub-steps represent numerical iterations (sometimes called sweeps) of the system of equations that represents the studied flow system. The need for a large number of time steps follows from the nature of a transient simulation, the larger the number of time steps the better the representation of the time-dependent evolution of the studied process; as long as no numerical difficulties occur because of a very short time step length (very short time steps may lead to truncation errors and also excessive computational times).

4.3 Cases exploring sensitivity to time step

We have carried out a series of simulations with different number of time steps, for the purpose of investigating the importance of the number and length of the time steps. These simulations are called numerical cases. The numerical cases are presented in Table 4-1. The only difference between the cases is the number of time-steps. The simulations were carried out for both the large and the small model. No numerical difficulties were observed for the studied cases.

Table 4-1. The different cases exploring the importance of the time step (numerical cases), simulated by use of the large and the small model.

Numerical case	Properties
1	Steps: 81. Sweep 5. Density dependent flow
2	Steps: 128. Sweep 5. Density dependent flow
3	Steps: 250. Sweep 5. Density dependent flow
4	Steps: 384. Sweep 5. Density dependent flow

4.4 Alternative Case 1: Hydrogeological properties

We have studied two different cases considering the hydrogeological properties of the flow medium. These cases are called the base case and the alternative case. The only difference between the two cases is the formulation of the depth dependency of the hydraulic conductivity. In the base case the depth dependency is defined as smoothly decreasing with depth, in the alternative case the depth dependency is defined as decreasing with depth by use of a step-function, see Section 2.6.2 and Figure 2-11. The results of the alternative Case 1 are presented in Section 4.9.

4.5 Alternative Case 2: No density effects

The above discussed base case has also been simulated without considering density effects, both for the small and the large models; this simulation is called alternative Case 2. The results of alternative Case 2 are presented in Section 4.10

4.6 Visualisation of calculated salinity distribution

The calculated distribution of the saline water (at 2,000 AD) is presented for Case 4 in a series of figures: Results of the large model is given in Figure 4-1, Figure 4-2 and Figure 4-4. Results of the small model is given in Figure 4-3 and Figure 4-5.

In the coordinate system of the established DT30 model, the centre of the studied repository is located at approximately X = 13,500 and Y = 44,500.

One conclusion that we may draw from the figures is that more of the saline water has been flushed out of the large model, compared to the small model. Hence, the flows are larger in the large model. This conclusion will be confirmed by the flow paths analyses.

4.7 Flow path analyses

In this study the flow pattern of the groundwater is analysed by the use of flow paths. The model create flow paths by simulating virtual particles that follow the flow of groundwater through the model (i.e. particle tracking). The flow paths represent advective flow only.

Particles were released in the calculated flow field of 2,000 AD. The flow field in which the particles moved was kept the same during the simulations of movement of the particles; hence in the model the shore line did not move during the simulation of the flow paths. The particles moved in a fixed flow field representing the flow situation at 2,000 AD. The particles were followed for a time period of 1 million years.

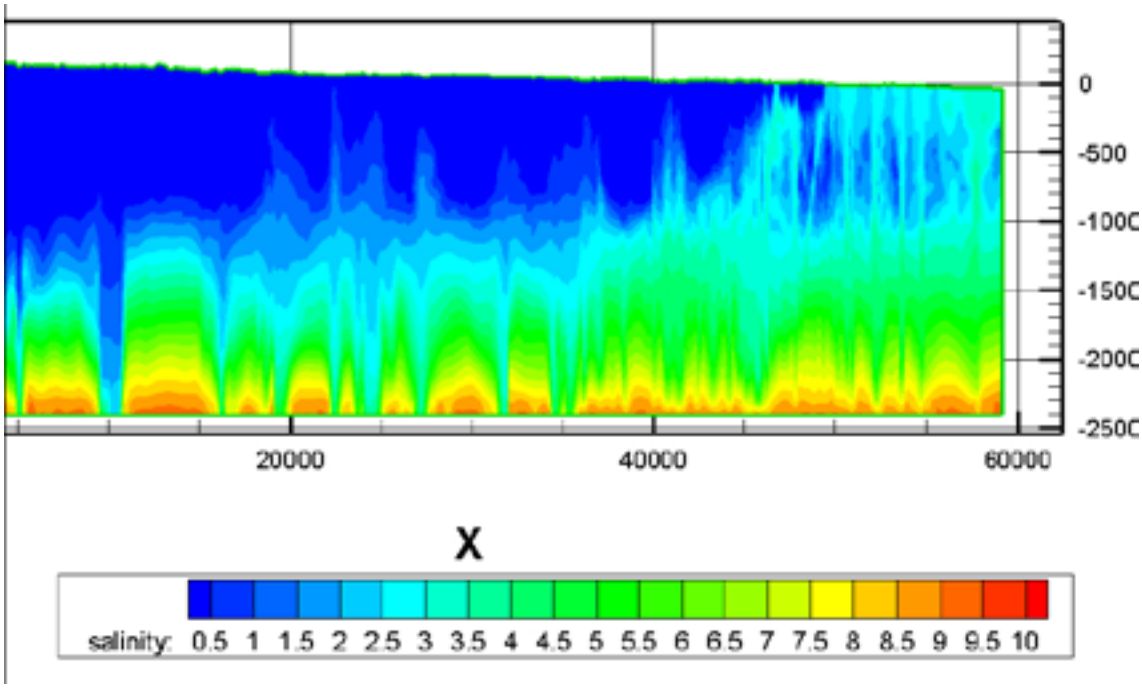

Figure 4-1. *Case 4. Results of simulation with large model. Time = 2,000 AD. Salinity distribution along a vertical cross-section from west to east, intersecting the repository area.*

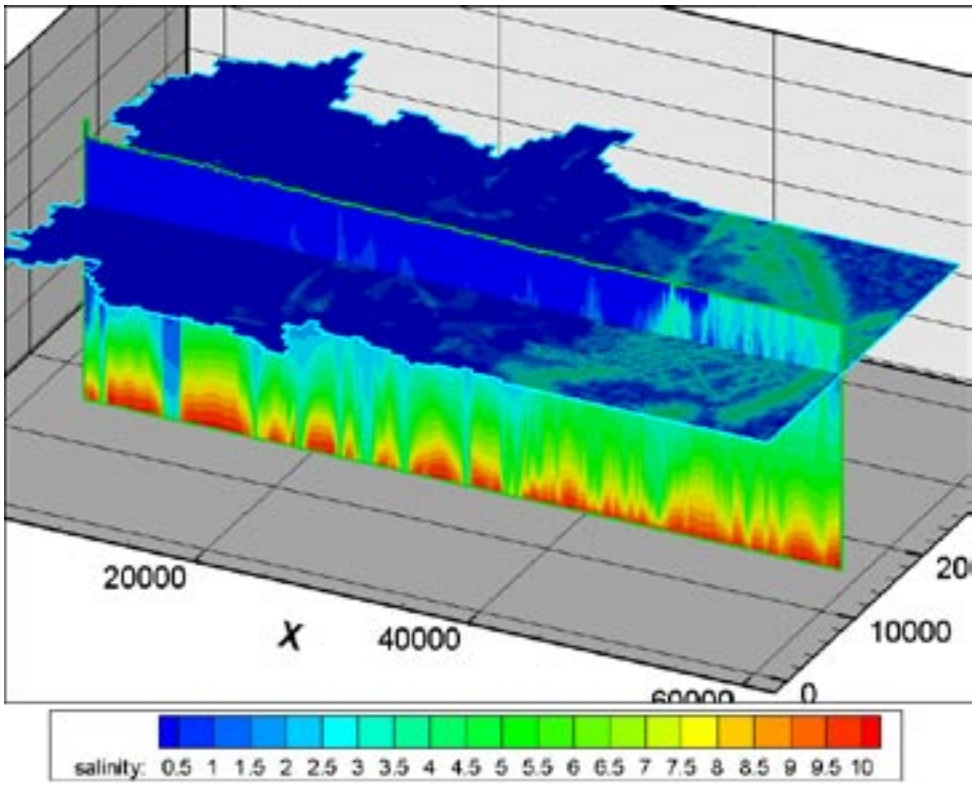

Figure 4-2. *Case 4. Results of simulation with large model. Time = 2,000 AD. Salinity distribution along a vertical cross-section from west to east, intersecting the repository area, and along a horizontal cross-section at an elevation of –500 m above sea level.*

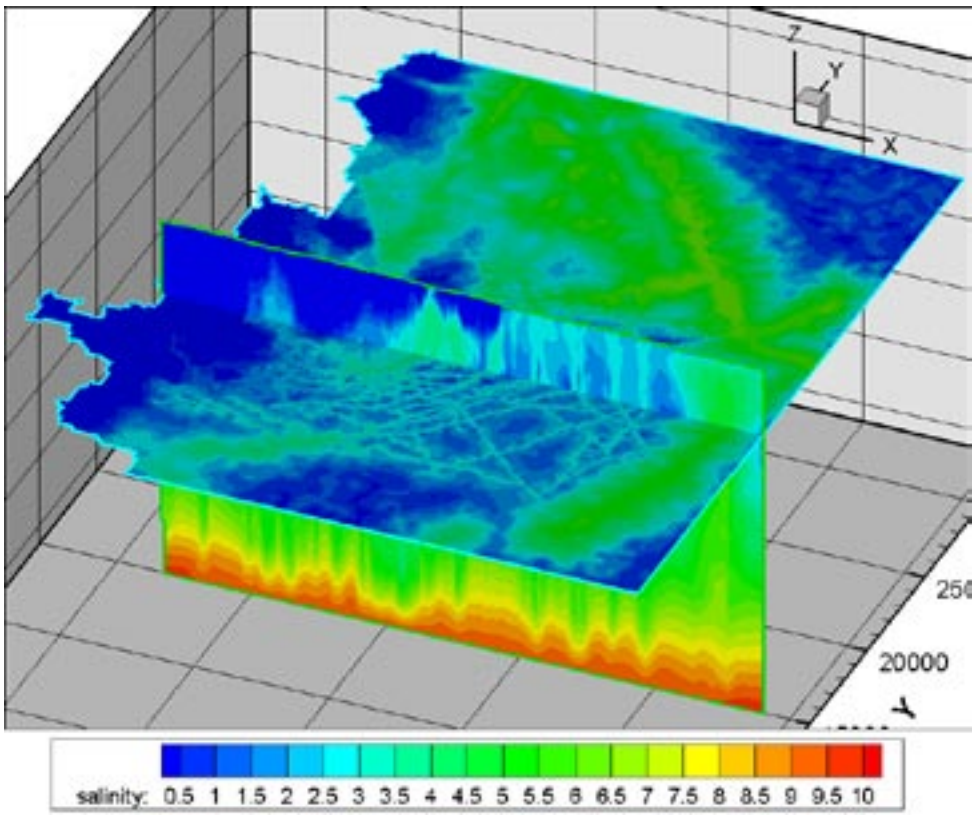

Figure 4-3. *Case 4. Results of simulation with small model. Time = 2,000 AD. Salinity distribution along a vertical cross-section from west to east, intersecting the repository area, and along a horizontal cross-section at an elevation of –500 m above sea level.*

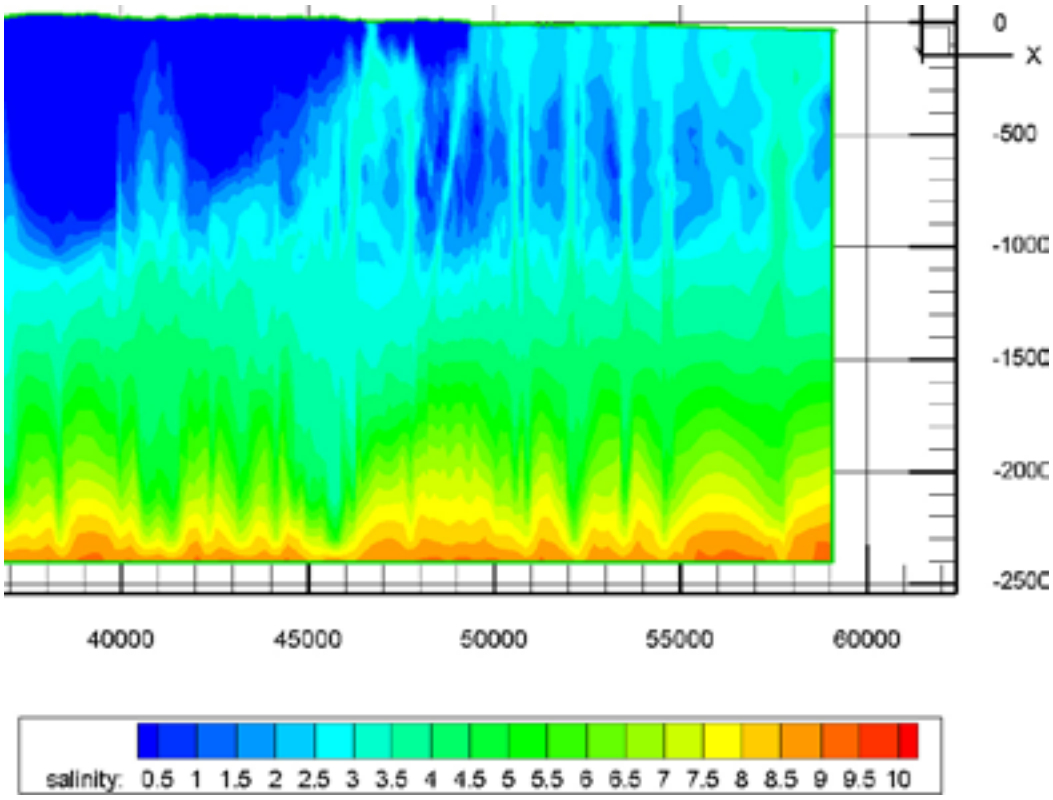

Figure 4-4. *Case 4. Results of simulation with large model. Time = 2,000 AD. Salinity distribution along a vertical cross-section from west to east, intersecting the repository area. The domain presented in the figure above corresponds approximately with the domain represented by the small model.*

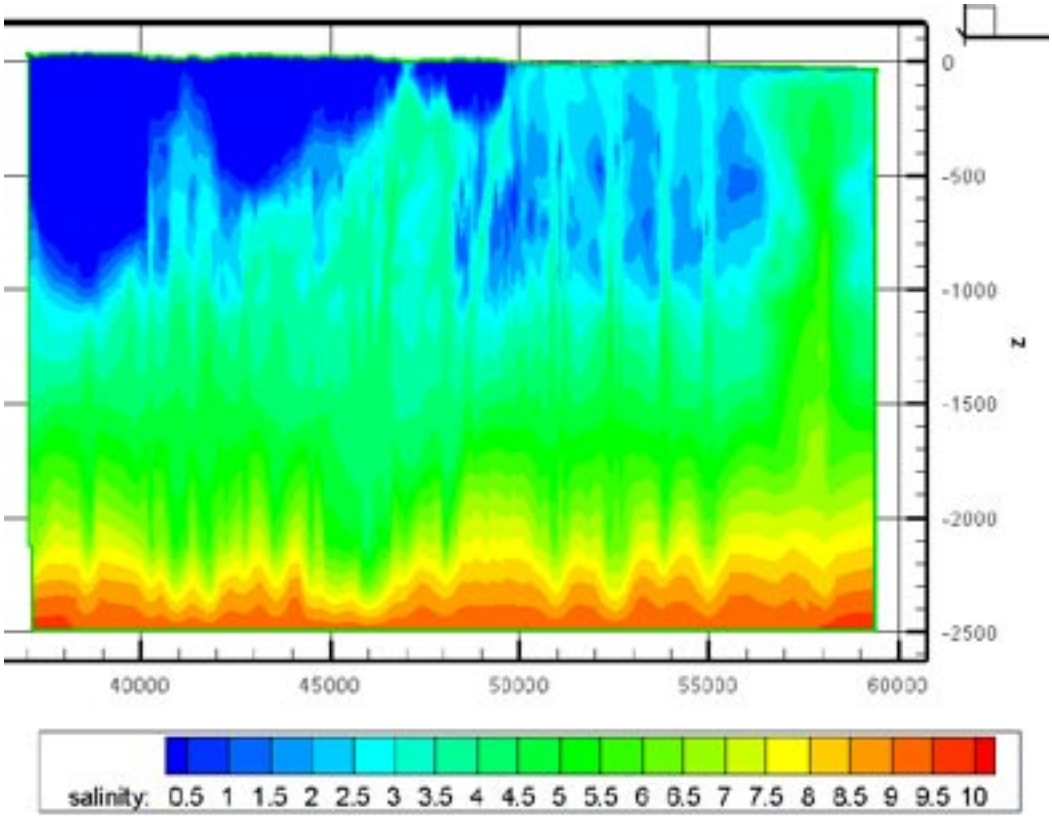

Figure 4-5. *Case 4. Results of simulation with small model. Time = 2,000 AD. Salinity distribution along a vertical cross-section from west to east, intersecting the repository area.*

The particles were released inside an area having the same extension as the Laxemar repository area (see Figure 4-6), at a depth of –500 m above sea level. The total number of particles released for each case studied is 1,737. Particles were released in a uniform pattern inside the repository area, regardless of fracture zones. Hence, particles were released primarily outside of fracture zones, but as the repository area is intersected by a few fracture zones, a few present of the particles were released inside fracture zones. Such particles will demonstrate short breakthrough times and large flows.

Length of flow paths

Length of flow paths are given in the following figures: Figure 4-7, Figure 4-8, Figure 4-9 and Figure 4-10. It is demonstrated by the figures that the lengths of the flow paths increase with number of time steps. The lengths obtained from the large model is however always *smaller* than the lengths obtained from the small model. (With one exception: For Case 2 above the 90th percentile the path-lengths of the small model is smaller than the lengths of the large model.) The case with the largest number of time steps (Case 4) demonstrates clearly that the path lengths are smaller for the large model.

Breakthrough time of flow paths

Breakthrough time of flow paths are given in the following figures: Figure 4-11, Figure 4-12, Figure 4-13 and Figure 4-14. It is demonstrated by the figures that the breakthrough times increase with number of time steps. The times obtained from the large model tend to be *smaller* than the times obtained from the small model. The case with the largest number of time steps (Case 4) demonstrates clearly that the breakthrough times are smaller for the large model.

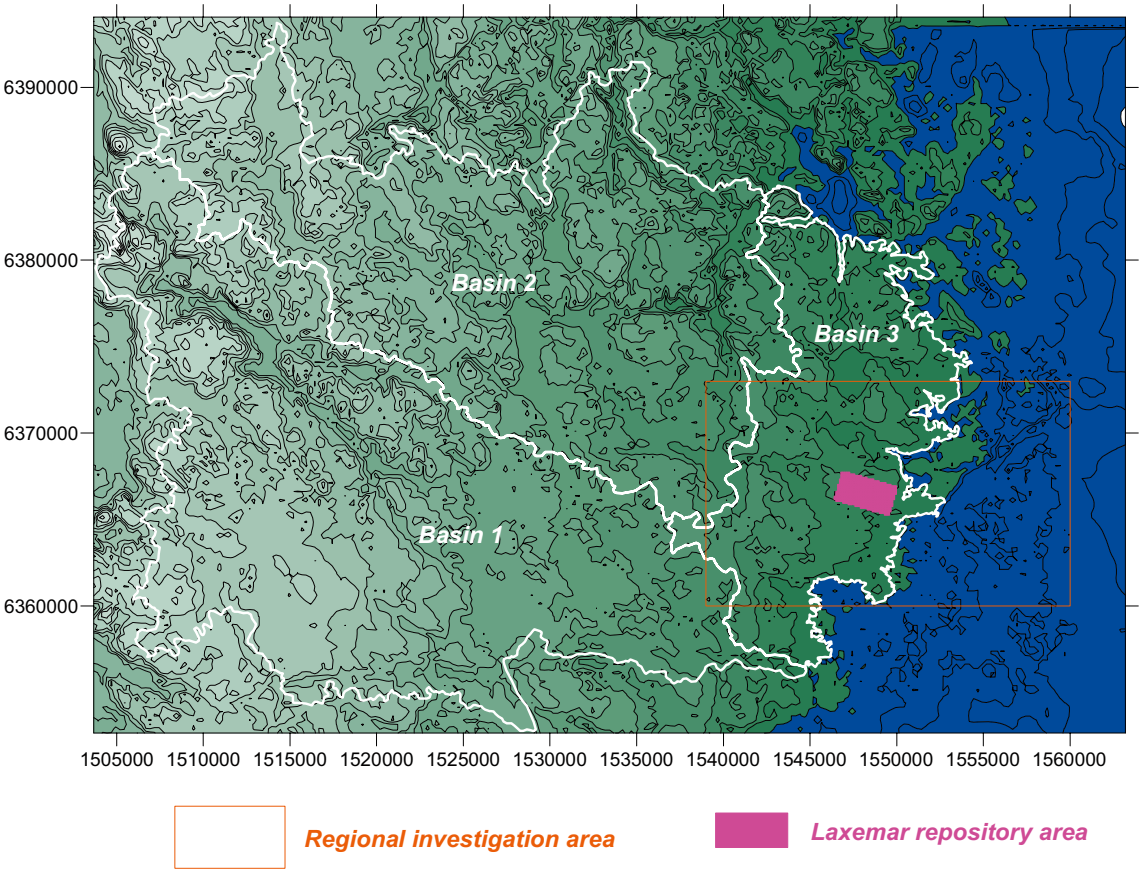

Figure 4-6. *Position of the Laxemar repository area (purple box). The particles were released inside this area at a depth of –500 m above sea level.*

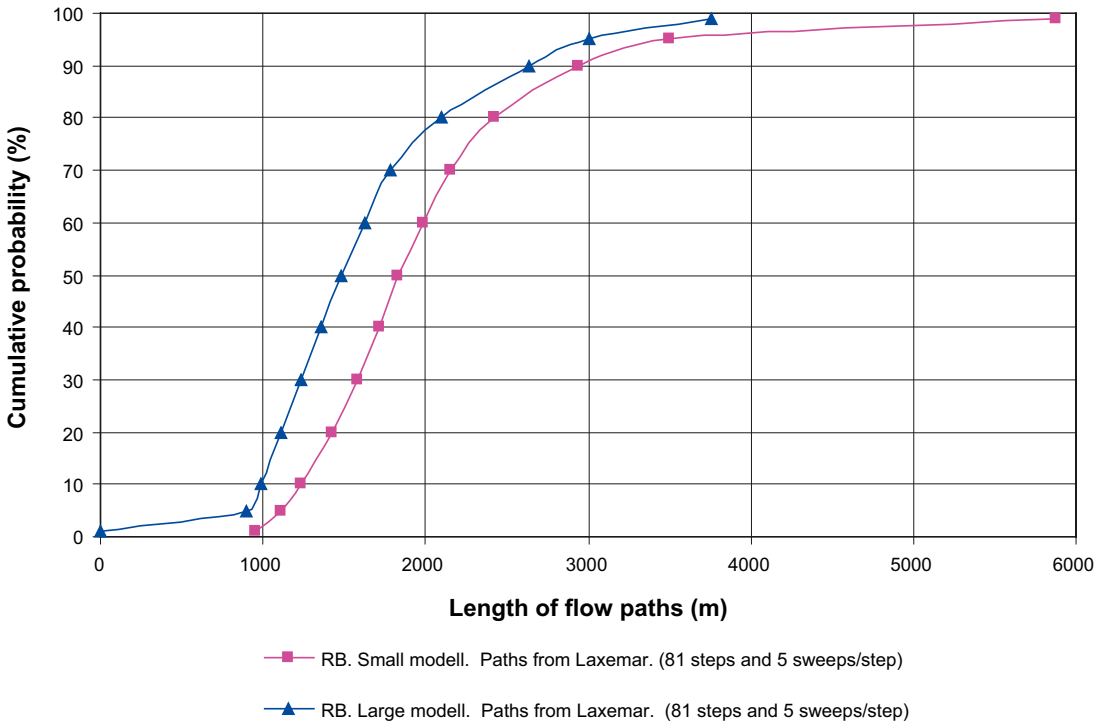

Figure 4-7. *Case 1: Length of flow paths.*

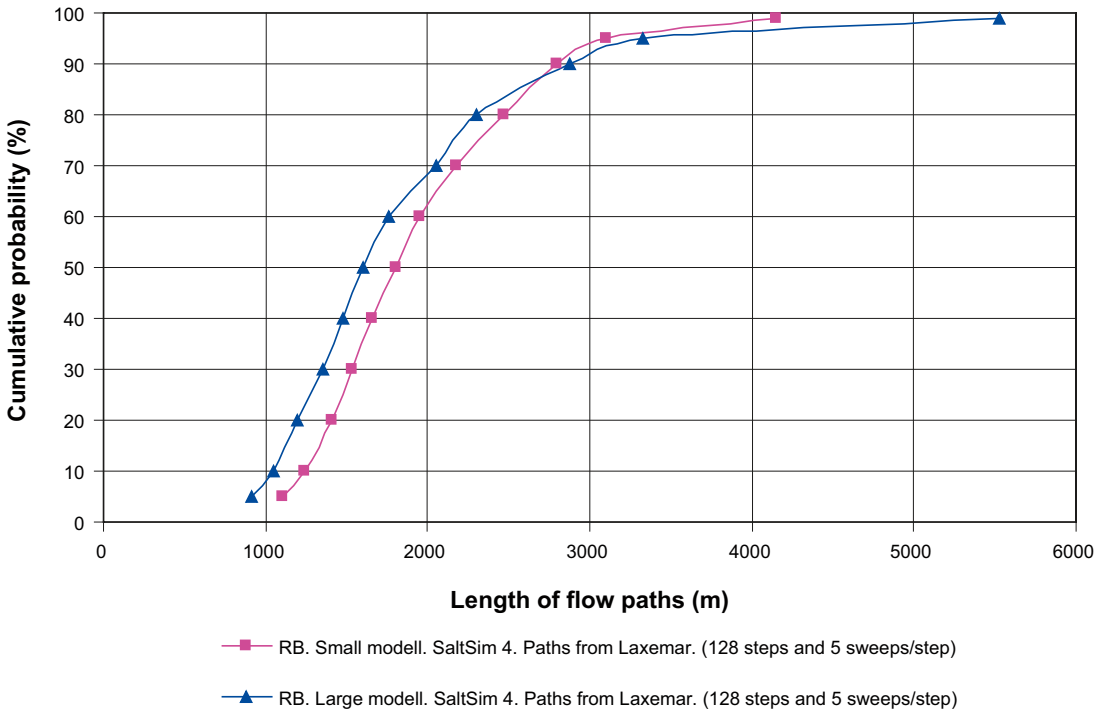

Figure 4-8. *Case 2: Length of flow paths.*

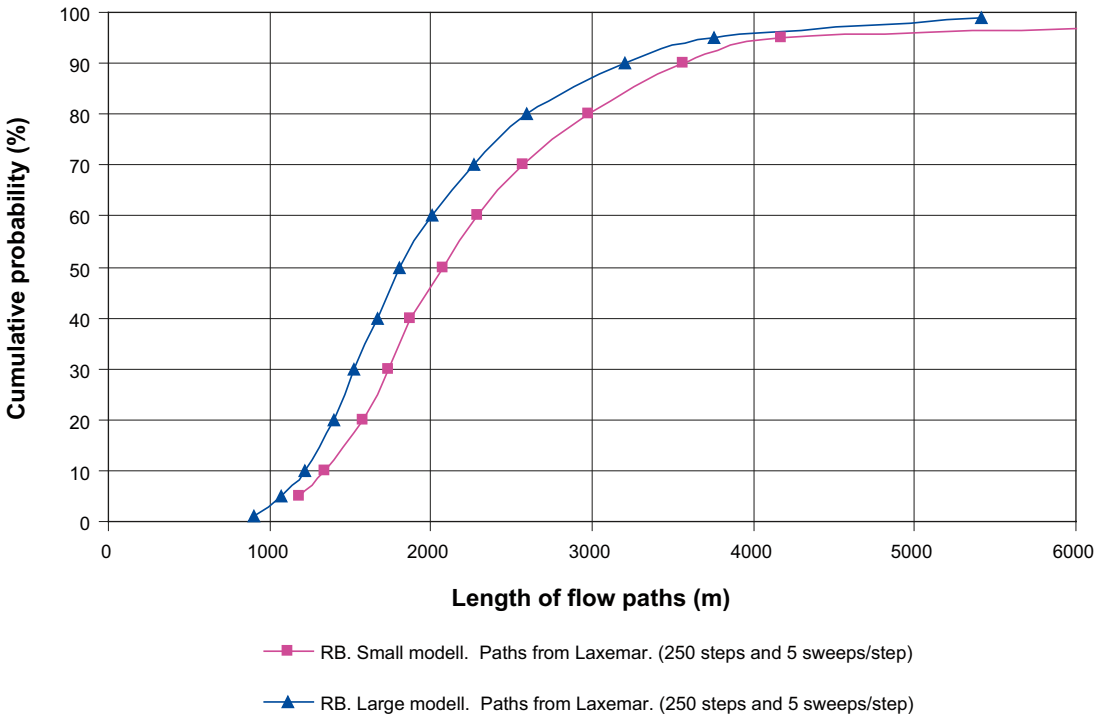

Figure 4-9. *Case 3: Length of flow paths.*

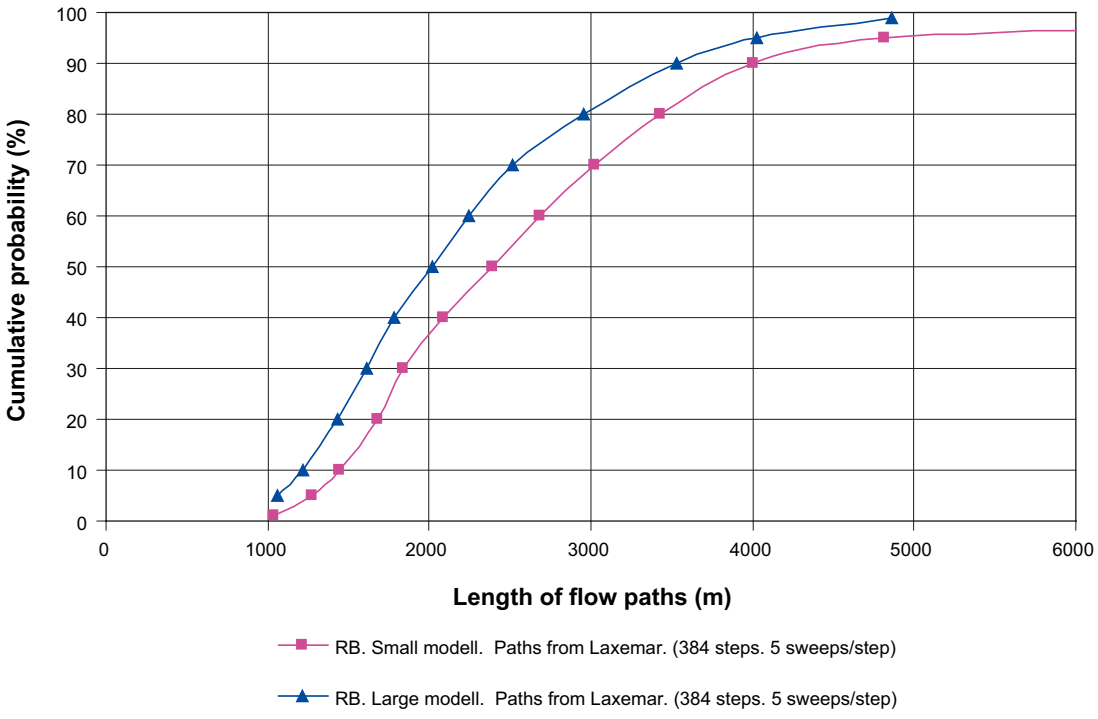

Figure 4-10. *Case 4: Length of flow paths.*

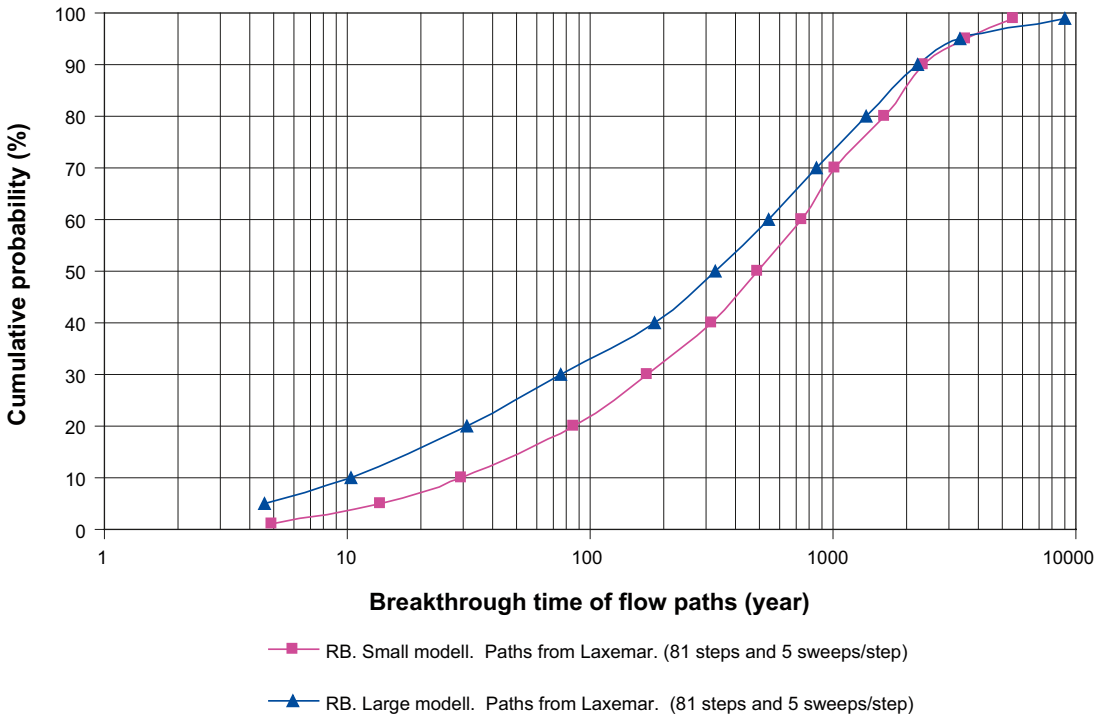

Figure 4-11. *Case 1. Breakthrough time of flow paths.*

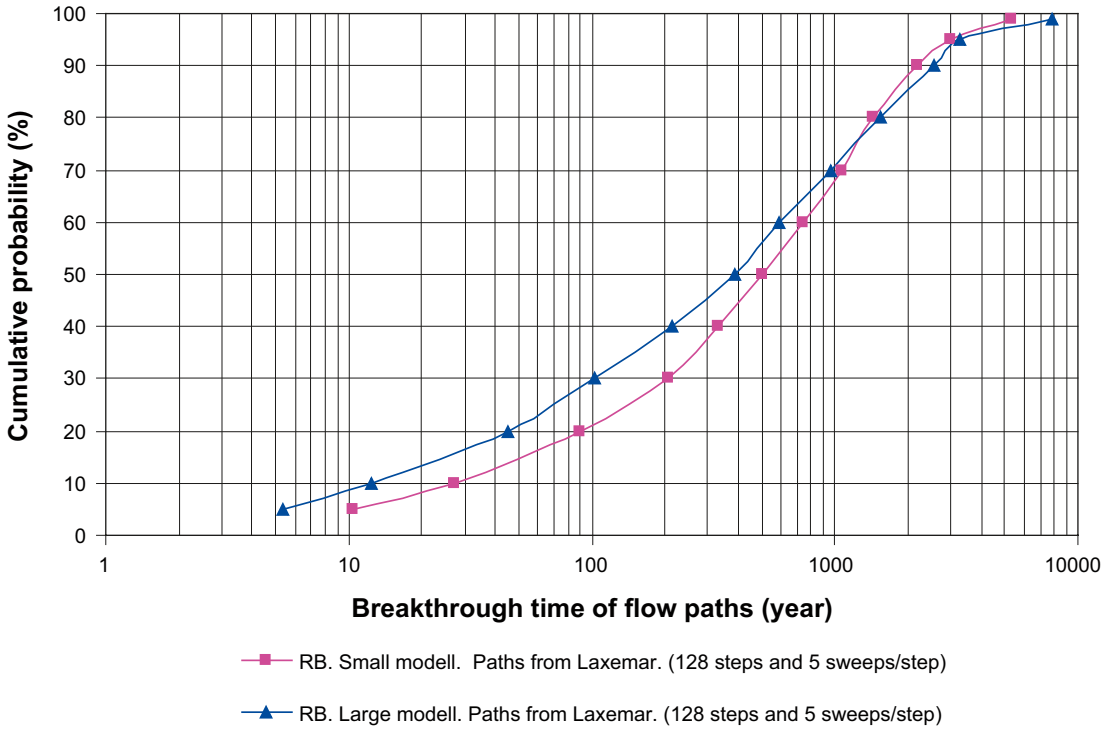

Figure 4-12. *Case 2. Breakthrough time of flow paths.*

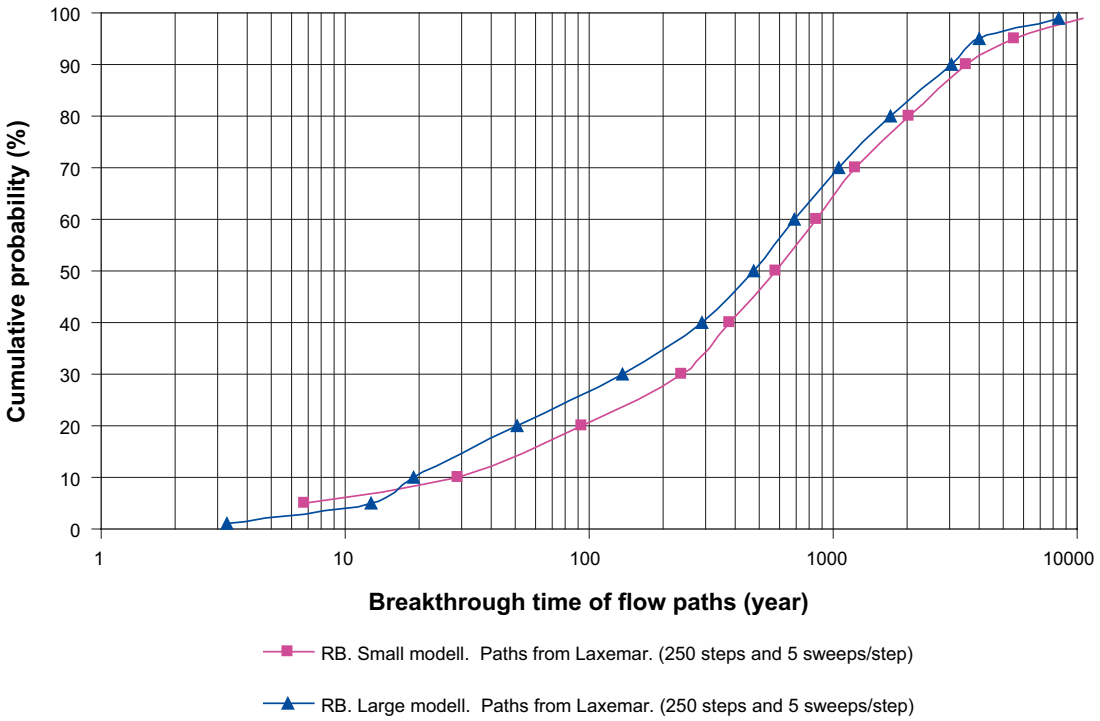

Figure 4-13. *Case 3. Breakthrough time of flow paths.*

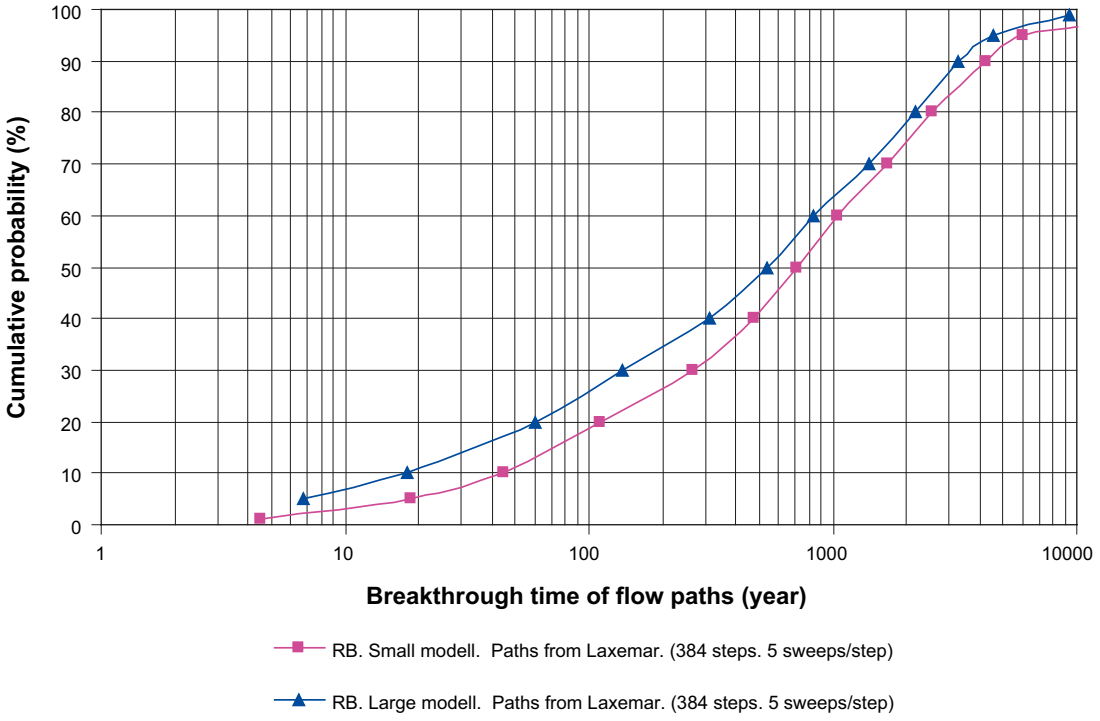

Figure 4-14. *Case 4. Breakthrough time of flow paths.*

Specific flow at start position (specific flow at repository area)

The specific flow at the start points of the flow paths, which is the same ting as the specific flow at repository depth, are given in the following figures: Figure 4-15, Figure 4-16, Figure 4-17 and Figure 4-18. It is demonstrated by the figures that the specific flows do not change much with increasing numbers of time steps. The flows obtained from the large model tend to be *larger* than the flows obtained from the small model. The case with the largest number of time steps (Case 4) demonstrates that the specific flows are larger for the large model. (Note the logarithmic scale.)

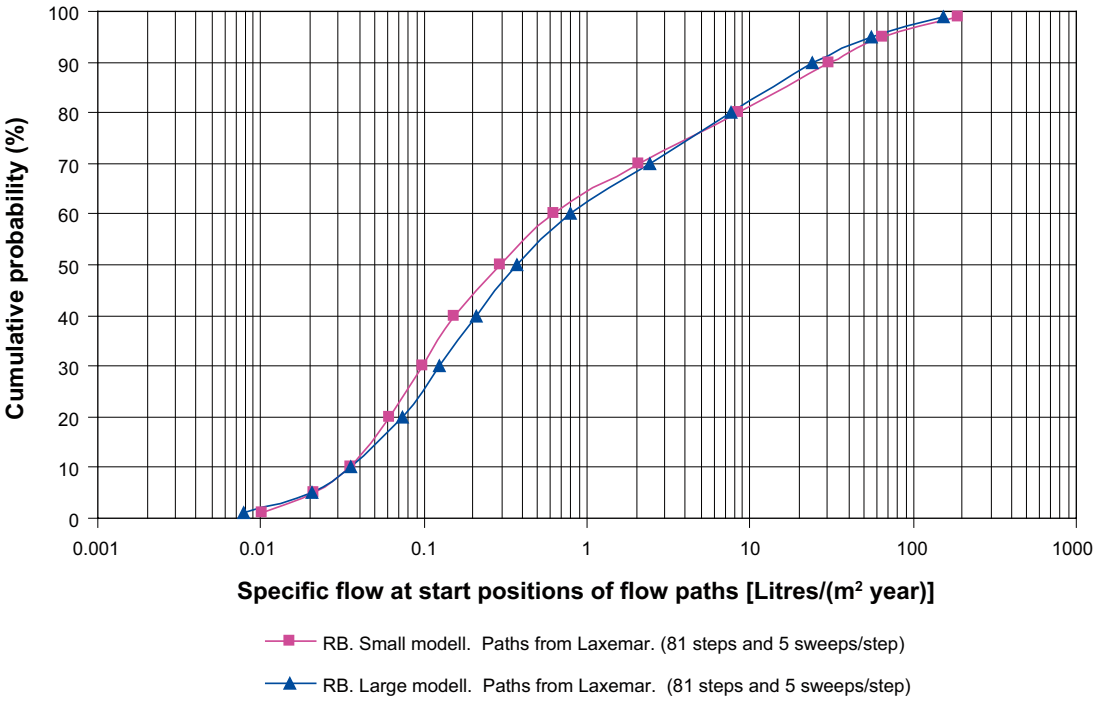

Figure 4-15. *Case 1. Specific flow at start positions.*

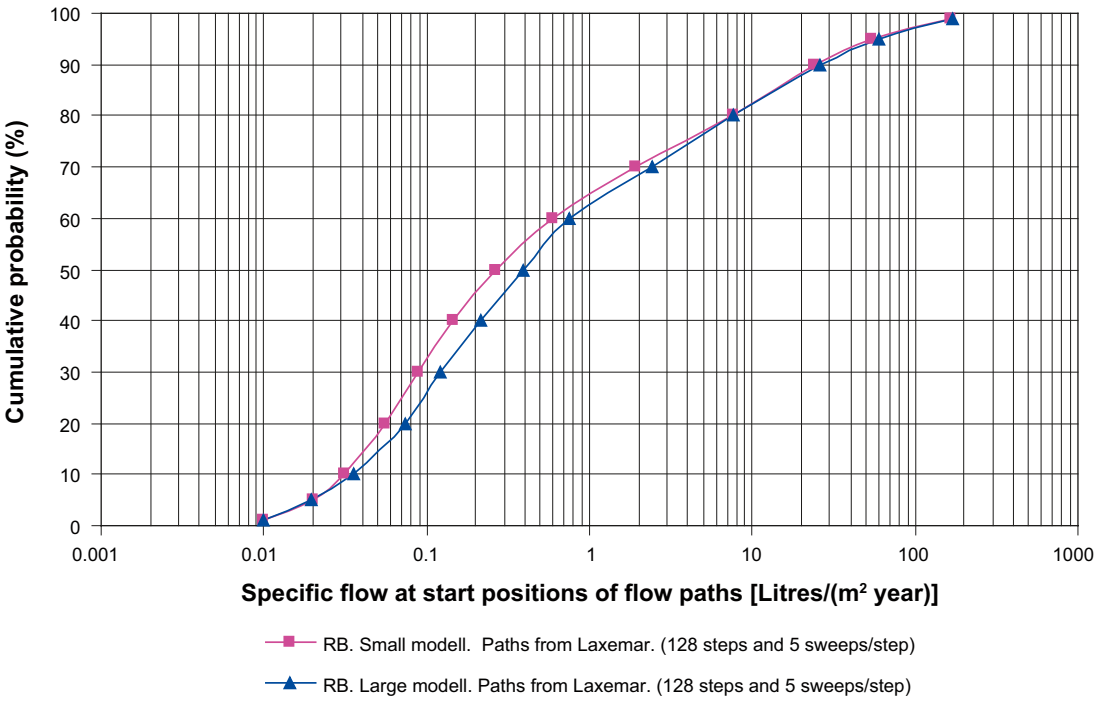

Figure 4-16. *Case 2. Specific flow at start positions.*

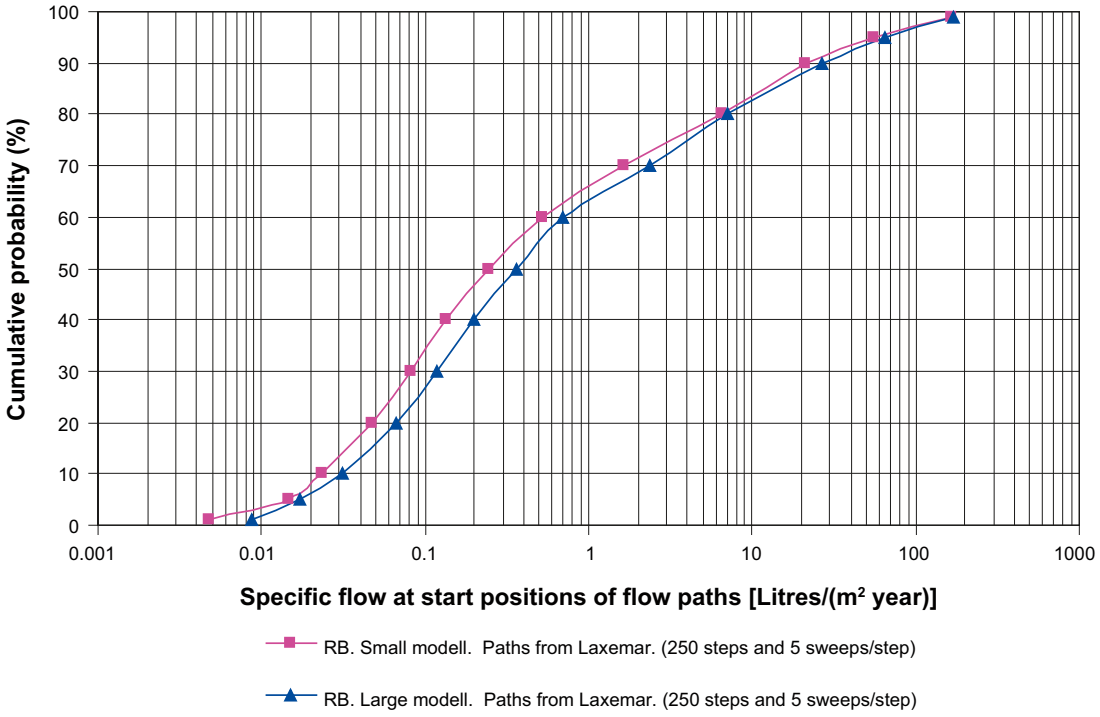

Figure 4-17. *Case 3. Specific flow at start positions.*

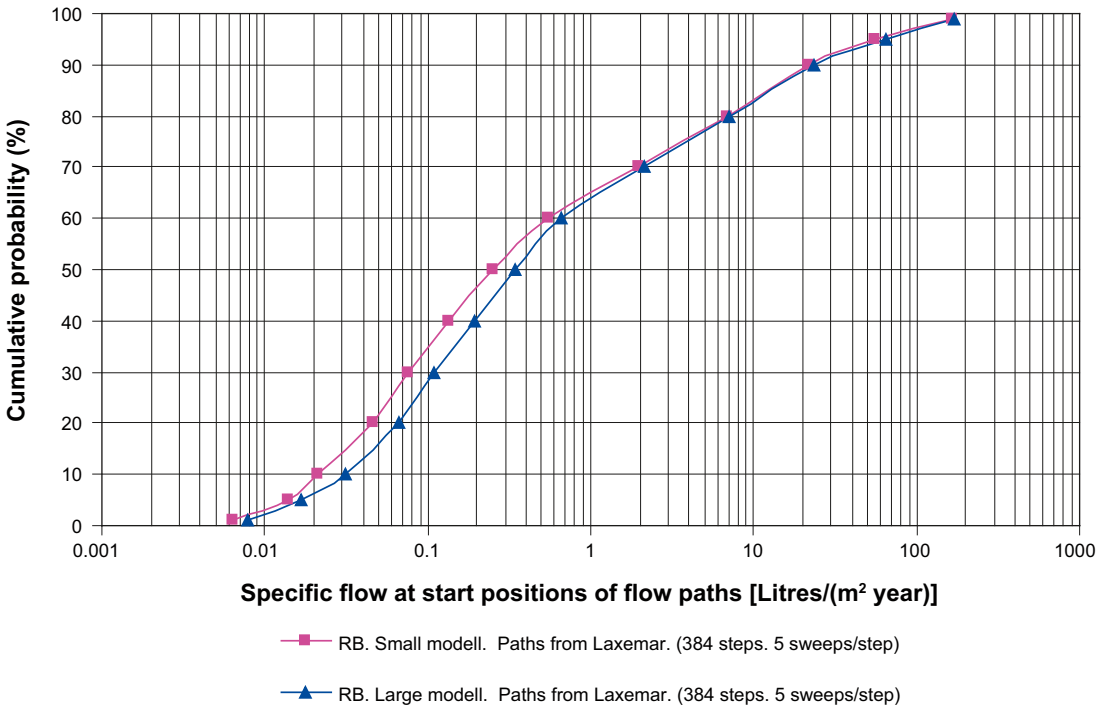

Figure 4-18. *Case 4. Specific flow at start positions.*

Detailed results for Case 4

Detailed results for the case with the largest number of time steps (Case 4) are given in Table 4-2 and Table 4-3: Particles were released in a uniform pattern inside the repository area, it follows that a few percent of the particles were released inside fracture zones, such particles will demonstrate short breakthrough times and large flows.

Table 4-2. Case 4. Large model. Detailed results of flow path analyses.

	Large model. Case 4.		
Percentiles	**Length [m]**	**Breakthrough time [years}**	**Specific flow [Litres/(m² year)]**
5	1,055	7	0.017
10	**1,217**	**18**	**0.031**
20	1,435	60	0.066
30	1,617	137	0.110
40	1,785	310	0.193
50	**2,018**	**541**	**0.347**
60	2,243	834	0.662
70	2,519	1,416	2.15
80	2,956	2,190	7.15
90	**3,528**	**3,272**	**23.49**
95	4,030	4,573	64.2
99	4,859	9,265	172.1

Table 4-3. Case 4. Small model. Detailed results of flow path analyses.

	Small model. Case 4.		
Percentiles	**Length [m]**	**Breakthrough time [years}**	**Specific flow [Litres/(m² year)]**
5	1,271	19	0.014
10	**1,441**	**45**	**0.021**
20	1,682	111	0.046
30	1,842	265	0.076
40	2,085	477	0.134
50	**2,396**	**717**	**0.248**
60	2,681	1,043	0.555
70	3,021	1,670	1.99
80	3,428	2,561	6.92
90	**4,004**	**4,233**	**21.8**
95	4,814	6,056	55.3
99	8,453	24,058	163.4

4.9 Comparison and discussion of results of flow path analyses

We have compared the results of the flow paths analyses (compared the distributions of values) obtained for the large and the small model, considering the case with the largest number of time steps (Case 4). The results are given in Table 4-4 (below).

It is demonstrated by Table 4-4 that for the 10th percentile the small model:

- Overestimates length of flow paths with a factor of 1.2.
- Overestimates breakthrough time of flow paths with a factor of 2.5.
- Underestimates the specific flow with a factor of 0.7.

It is demonstrated by Table 4-4 that for the median values the small model:

- Overestimates length of flow paths with a factor of 1.2.
- Overestimates breakthrough time of flow paths with a factor of 1.3.
- Underestimates the specific flow with a factor of 0.7.

It is demonstrated by Table 4-4 that for the 90th percentile the small model:

- Overestimates length of flow paths with a factor of 1.1.
- Overestimates breakthrough time of flow paths with a factor of 1.3.
- Underestimates the specific flow with a factor of 0.9.

The small model underestimates the size of the groundwater flow; the underestimation follows from the limited size of the small model and the weakly developed surface water divide used as the westernmost boundary condition of the small model. (This surface water divide is marked in Figure 2-3 with a purple line.)

The location of the westernmost boundary of the models is of importance as the regional flow of groundwater is primarily from the west towards the sea (as given by the regional topography).

The weakly developed surface water divide is conceptually applied in the small model as a groundwater divide; in the small model it is represented by a no-flow boundary condition.

Table 4-4. Results of comparisons of flow path analyses.

	Comparisons of results obtained for large and small flow models. The comparisons are presented by use of factors: Factor = [Result from small model]/[Result from large model]		
Percentiles	**Length**	**Breakthrough time**	**Specific flow**
5	1.20	2.77	0.82
10	**1.18**	**2.47**	**0.69**
20	1.17	1.85	0.69
30	1.14	1.93	0.69
40	1.17	1.54	0.69
50	**1.19**	**1.33**	**0.72**
60	1.20	1.25	0.84
70	1.20	1.18	0.92
80	1.16	1.17	0.97
90	**1.13**	**1.29**	**0.93**
95	1.19	1.32	0.86
99	1.74	2.60	0.95

The simulation with the large model demonstrates however that the weakly developed surface water divide is not a groundwater divide for the groundwater flow at large depths.

It follows that the deep groundwater flow that passes below the weakly developed surface water divide will not be included in the small model.

As this deep groundwater flow is not included in the small model, the small model will underestimate the groundwater flows at the repository depth, and overestimate lengths of flow paths as well as the breakthrough times of flow paths from the repository area. The differences when comparing the flow paths properties are however not large because the flows at large depths are small.

When the deep groundwater flow is included in the model, as in the large model, the discharge of groundwater close to the shoreline is somewhat larger than in the small model, and at 2,000 AD less of the saline water will occur in the large model at repository depths. A comparison of the flow pattern in the small and in the large model indicates the when the deep groundwater flow is included the flow paths (from the tentative repository) tend to follow flow routs with shorter horizontal extensions than in the small model. In addition, in the large model less flow paths will move downwards at the starting positions and the vertical extension (downwards) of the flow paths will also be less pronounced than in the small model.

The reason for the overestimation of breakthrough times in the small model (compared to the large model) is that the flow paths are somewhat shorter in the small model and the magnitudes of the flows are somewhat smaller as well.

4.10 Results of alternative Case 1. Hydrogeological properties

As previously discussed, we have studied two different cases considering the hydrogeological properties of the flow medium. The only difference between the two cases is the formulation of the depth dependency of the hydraulic conductivity. In the base case the depth dependency is defined as smoothly decreasing with depth, in the alternative Case 1 the depth dependency is defined as decreasing with depth by use of a step-function, see Section 2.6.2 and Figure 2-11.

The simulation of the alternative Case 1 was carried out with similar numerical settings as for numerical Case 1, see Table 4-1. A comparison of the results of the flow path analyses, comparing the small and large models of the alternative case, is given below.

Alternative Case 1 demonstrates the following results:

For the median values the small model:

- Overestimates length of flow paths with a factor of 1.2.
- Overestimates breakthrough time of flow paths with a factor of 1.4.
- Underestimates the specific flow with a factor of 0.7.

Hence, the differences between the small and the large model are approximately the same for the base case and for the alternative case. The results of alternative Case 1 confirm the results of the base case.

4.11 Results of alternative Case 2. No density effects

Simulations without density effects were carried out both for the large and the small model, flow paths were released in both models and the results were compared in the same way as for the cases discussed above.

The simulations without density effects demonstrate the same principle behaviour as the cases with density effects, although some of the differences between the large and the small model are larger when density effects are not included. Without density effects the groundwater flows at large depths (the deep groundwater flow) will be larger than if density effects are included.

If density effects are included in the models, the heavy saline water at great depths will not move as easy in response to the retreating shore line, the undulation of the groundwater surface and the changing pressures close to the ground surface, in comparison to a situation in which there are no density effects and the water at great depths has the same weight as the groundwater close to the ground surface. The heavy saline water at great depths will limit the magnitude of the deep groundwater flow.

The differences in results between the large and the small models follow from the deep groundwater flows, which are not fully included in the small model. The deep groundwater flows are larger in a model without density effects and the differences in flow path lengths and flow path breakthrough times are larger as well when comparing results from the large and the small model (for simulations without density effects).

The larger flows in the model without density effects can be illustrated by comparing the specific flow at the start positions of the flow paths for the large model with and without density effects. The median specific flow is 1.6 times larger in the large model without density effects, in comparison to the large model with density effects.

Alternative Case 2 demonstrates the following results:

For the median values the small model:

- Overestimates length of flow paths with a factor of 2.9.
- Overestimates breakthrough time of flow paths with a factor of 2.5.
- Underestimates the specific flow with a factor of 0.95.

We note that the difference in specific flow is not as large as the differences in length of flow paths and breakthrough time of flow paths, when comparing the small and the large model.

The results of alternative Case 2 confirm the results of the base case.

5 Conclusions

The location of the westernmost hydraulic boundary of a regional groundwater flow model representing the Laxemar investigation area is of importance as the regional flow of groundwater is primarily from the west towards the sea (as given by the regional topography). If the westernmost boundary condition of a regional flow model is located to close to the investigation area, the regional flow model may underestimate the magnitude of the regional groundwater flow (at the investigation area), as well as overestimate breakthrough times of flow paths from the repository area, etc.

The objective of this study is to calculate and compare the groundwater flow at a tentative repository area at Laxemar; for a very large groundwater flow model, much larger than the regional flow model used by /Hartley et al. 2006/ (SKB R-06-23 Site description version 1.2), as well as for a flow model that is of comparable size to the regional model used by /Hartley et al. 2006/.

The comparisons include the following three parameters:

- Length of flow paths from the tentative repository area.
- Advective breakthrough time for flow paths from the tentative repository area.
- Magnitude of flow at the tentative repository area.

The comparisons demonstrated the following considering the median values of the obtained distributions of flow paths properties.

The small model:

- Overestimates length of flow paths with a factor of 1.2
- Overestimates breakthrough time of flow paths with a factor of 1.3
- Underestimates the specific flow with a factor of 0.7

The small model underestimates the size of the groundwater flow; the underestimation follows from the limited size of the small model and the weakly developed surface water divide used as the westernmost boundary condition of the small model.

The weakly developed surface water divide is conceptually applied in the small model as a groundwater divide; in the small model it is represented by a no-flow boundary condition.

The simulation with the large model demonstrates however that the weakly developed surface water divide is not a groundwater divide for the groundwater flow at large depths. It follows that the deep groundwater flow that passes below the weakly developed surface water divide will not be included in the small model. As this deep groundwater flow is not included in the small model, the small model will underestimate the groundwater flows at the repository area, and overestimate lengths of flow paths as well as the breakthrough times of flow paths from the repository area. The differences when comparing the flow paths properties (as calculated by the large and small models) are however not large; because the deep groundwater flow that is missing in the small model is not large.

6 References

Carlsson L, Gustafsson G, 1984. Provpumpning som geohydrologisk undersökningsmetodik. Byggforskningsrådet R41:1984.

EU RETROCK, 2005. RETROCK 2005, Treatment of geosphere retention phenomena in safety assessments. Final report of the RETROCK Concerted Action, Work performed as part of the European Atomic Energy Community's (Euratom) framework of the specific research and training programme. Contract No FIKW-CT-2001-20201, EUR 21230EN, European Commission.

Ericsson L O, Holmén J G, Rhén I, Blomquist N, 2006. Storregional grundvattenmodellering – fördjupad analys av flödesförhållanden i östra Småland. Jämförelse av olika konceptuella beskrivningar. SKB R-06-64 (report in Swedish, summary in English), Svensk Kärnbränslehantering AB.

Follin S, Svensson U, 2003. On the role of mesh discretisation and salinity for the occurrence of local flow cells. Results from a regional-scale groundwater flow model of Östra Götaland. SKB R-03-23, Svensk Kärnbränslehantering AB.

Follin S, Stigsson M, Svensson U, 2005. Regional hydrogeological simulations of Forsmark – numerical modelling using DarcyTools. Preliminary site description. Forsmark area – version 1.2. SKB R-05-60, Svensk Kärnbränslehantering AB.

Haggerty R, Gorelick S M, 1995. Multi-rate mass transfer for modelling diffusion and surface reactions in media with pore-scale heterogeneity. Water Resources Research, 31(10), pp 2383–2400.

Hartley L, Hunter F, Jackson P, McCarthy R, 2006. Regional hydrogeological simulations using CONNECTFLOW. Preliminary site description. Laxemar subarea – version 1.2. SKB R-06-23, Svensk Kärnbränslehantering AB.

Holmén J G, 1997. On the flow of groundwater in closed tunnels. Generic hydrogeological modelling of nuclear waste repository, SFL 3–5. SKB TR 97-10, Svensk Kärnbränslehantering AB.

Holmén J G, Stigsson M, Marsic N, Gylling B, 2003. Modelling of groundwater flow and flow paths for a large regional domain in northeast Uppland. SKB R-03-24, Svensk Kärnbränslehantering AB.

Rhén I, Forsmark T, Forssman I, Zetterlund M, 2006. Evaluation of hydrogeological properties for Hydraulic Conductor Domains (HCD) and Hydraulic Rock Domains (HRD), Preliminary site description, Laxemar subarea – version 1.2. SKB R-06-22. Svensk Kärnbränslehantering AB.

SNA, 1994. Sveriges Nationalatlas (SNA): Berg och jord. SGU 1994.

Svensson U, Kuylenstierna H-O, Ferry M, 2004. DarcyTools, Version 2.1. Concepts, methods, equations and demo simulations. SKB R-04-19, Svensk Kärnbränslehantering AB.

Voss C I, Provost A M, 2001. Recharge-area nuclear waste repository in Southeastern Sweden, Demonstration of hydrogeologic siting concepts and techniques, SKI rapport 01:44, Stockholm.

Appendix A

Definition of heterogeneity

The flow medium studied is a fractured rock. Groundwater flow in such a rock occurs in fractures and in fracture zones of different size and significance. As the conductivity of a fractured rock depends on a large number of connected fractures having different properties, the conductivity of fractured rock becomes heterogeneous, anisotropic and scale dependent.

There are different approaches available when establishing a mathematical description of a fractured rock mass. The continuum approach (also called the Continuous Porous Medium approach – CPM) is often used; the CPM approach replaces the fractured medium by a representative continuum in which spatially defined values of hydraulic properties can be assigned to blocks of a given size. The CPM approach is used in this study. The heterogeneity of the flow medium is introduced to the CPM models by defining the permeability of a cell (block) of the computational grid by use of probability distributions. Field tests have demonstrated that the permeability of rock blocks may be described by non-symmetrical probability distributions, such as the Log-Normal distribution. (This is also confirmed by theoretical discrete fracture network modelling.) The introduction of stochastic values of permeability will produce a stochastic continuum model (a stochastic CPM model).

The difficulty with the stochastic continuum approach is the selection of probability distributions. Observations in the field (e.g. at Äspö Hard Rock Laboratory) have demonstrated that the heterogeneity of the permeability field is scale dependent.

The scale dependency for a heterogeneous three dimensional volume may be described as follows: at small scales the heterogeneity is large (different small rock blocks may have very different values of permeability) and at large scales the heterogeneity is small (different large rock blocks may have approximately the same permeability), presuming that the studied domain is statistically homogeneous (see below).

The description of a heterogeneous permeability as given above assumes statistical homogeneity: by statistical homogeneity we mean that the general statistical properties (parameters) of the heterogeneity of the rock domain studied are the same regardless of position of a rock block within the rock domain; or with other words that all samples (rock blocks) are taken from the same population (rock domain).

It is also a property of the scale dependency (within a statistical homogeneous domain) that the mean (geometric mean or median) permeability of heterogeneous rock blocks (three dimensions) increases with size of rock block, or with other words:

- A sample of small heterogeneous rock blocks will demonstrate a small mean permeability but a large variation in permeability values.
- A sample of large heterogeneous rock blocks will demonstrate a large mean permeability but a small variation in permeability values.

It follows from the discussion above that the permeability of heterogeneous rock blocks will asymptotically tend to an effective value at large scale.

In the discussion above we mentioned the concept of an *effective value* of a heterogeneous permeability field. The effective values should not be confused with an *equivalent value*.

Equivalent conductivity: By equivalent conductivity we mean a hydraulic conductivity tensor representing a heterogeneous flow medium at a given scale and for a given flow direction. The equivalent conductivity will change with scale. A complete equivalence between a heterogeneous medium and a homogeneous ‘average’ representation is impossible; the concept of an equivalent conductivity is only applicable under certain conditions.

Effective conductivity: For some flow systems, considering an average flow direction and certain types of heterogeneity (e.g. for a stochastic continuum model), the equivalent conductivity will tend to a certain value at large scales; by an effective conductivity we mean an equivalent conductivity taken at such a large scale that for even larger scales the scale dependency in conductivity is insignificant.

Considering a flow medium defined as a statistical homogeneous stochastic continuum, a flow medium that consists of a large number of sub-volumes (rock blocks or cells) with isotropic conductivity values as given by a Log-Normal distribution, for such a medium and for an average uniform flow, /Landau and Lifshitz 1960/ as well as /Matheron 1967/ have proposed analytical solutions for calculation of the effective conductivity. The analytic solutions define the effective conductivity value as a function of the mean conductivity and of the standard deviation of the Log-Normal distribution defining the conductivity of the sub-volumes (rock-blocks or cells).

In this study the selected heterogeneity, for each lithological unit and fracture zone, is based on the variation in K-values as demonstrated in the Water well archive of SGU, and in the variation observed at the site investigations.

In this study the heterogeneity is defined separately for each lithological unit and fracture zone, by use of a method presented in /Holmén 1997/. For each lithological unit and fracture zone, the heterogeneity at different scales is defined by an interpolated and conditioned function that represents the average K-values of the lithological unit or fracture zone, and also produces the same effective conductivity of the heterogeneous flow medium regardless of scale studied. This condition is achieved by application of the analytical theories by /Matheron 1967/. The method for interpolation is discussed in more detail in /Holmén 1997/. The method is also consistent with the internal scale dependency that is a part of all stochastic continuum models. The equations defining the scale dependency is given below as Equation A-1 (see also Figures A-1 and A-2).

It is important to apply a method for generation of heterogeneity that is consistent with the concepts of a stochastic continuum and an effective hydraulic conductivity. The concept of an effective conductivity is important as the effective value is the bridge between models with and without a stochastic heterogeneity.

For each lithological unit and fracture zone, the heterogeneity is generated as follows:

1. Effective values are derived based on available data and for different depths (see Figure 2-7 and Table 2-2, and Section 2.7)
2. Each cell of the mesh is assigned a Log-Normal conductivity distribution, the geometric mean of this distribution and standard deviation is calculated in a way that the heterogeneity is in line with the observed data and also in a way that the effective value of a stochastic continuum corresponds to the selected value. (See Equation A-1 and Figures A-1 and A-2)
3. Each cell is given a random value of conductivity as defined by the Log-Normal probability distribution assigned to that cell.

The established model includes cells of different sizes therefore the probability distributions that defines the varying permeability of the cells will be different for cells of different sizes (scale dependency). The probability distributions will also vary with depth (depth dependency). And the probability distributions will also be different for the different lithological units and fracture zones.

References

Holmén J G, 1997. On the flow of groundwater in closed tunnels. Generic hydrogeological modelling of nuclear waste repository, SFL 3–5. SKB TR 97-10, Svensk Kärnbränslehantering AB.

Landau L D, Lifshitz E M, 1960. Electrodynamics of continuous media. Pergamon, Oxford.

Matheron G, 1967. Eléments pour une théorie des milieux poreux. Masson, Paris, France.

Equation A-1.

Functions defining scale dependency, used in stochastic continuum models

Geometric mean of Log-Normal distribution defining conductivity of rock blocks, an interpolated curve. Curve (A) ass given in Figure A-1:

$$K_{BG} = \frac{2\left(a\tan(X)^{P_2}\right) - a\tan(P_1)^{P_2}}{a\tan(P_1)^{P_2}} \quad \frac{a\tan(X\ P_3)}{a\tan(P_1\ P_3)} \quad \frac{X^{P_4}}{P_1^{P_4}} \quad K_E$$

Standard deviation (in eLog space) of Log-Normal distribution defining conductivity of rock blocks /Matheron 1967/. Curve (B) as given in Figure A-1:

$$\sigma_{eLog\ KB} = \sqrt{6\,eLog\left(\frac{K_E}{K_{BG}}\right)}$$

K_E = *Effective conductivity of the flow domain represented by a stochastic continuum.*

K_{BG} = *Log-normal block conductivity distribution: Geometric mean of the distribution.*

$\sigma_{eLog\ KB}$ = *Log-normal block conductivity distribution: Standard deviation of the natural logarithms of the distribution (STD of eLog* K_{block}*).*

X = *Scale of field measurements as well as scale of blocks in stochastic continuum model.*

Curve fitting parameters

P_1 = *Curve fitting parameter, corresponding to the block size for which the standard deviation of the block conductivity is set to zero.*

P_2 = *Curve fitting parameter.*

P_3 = *Curve fitting parameter.*

P_4 = *Curve fitting parameter.*

Parameters defining curve: A

	P_1	P_2	P_3	P_4	K_E
Curve B	*1,000*	*2.65*	*0.14*	*0.5*	*As defined by the given parameter distributions, see Table 2-2*

The model includes cells of varying size; the scale of the cells is defined by the side of a cube having a volume equal to the volume of the cells, as defined below (Cartesian coordinate system):

$$X = \sqrt[3]{C_x\ C_y\ C_Z}$$

C_x = *Length of cell in X-direction*

C_y = *Length of cell in Y-direction*

C_z = *Length of cell in Z-direction*

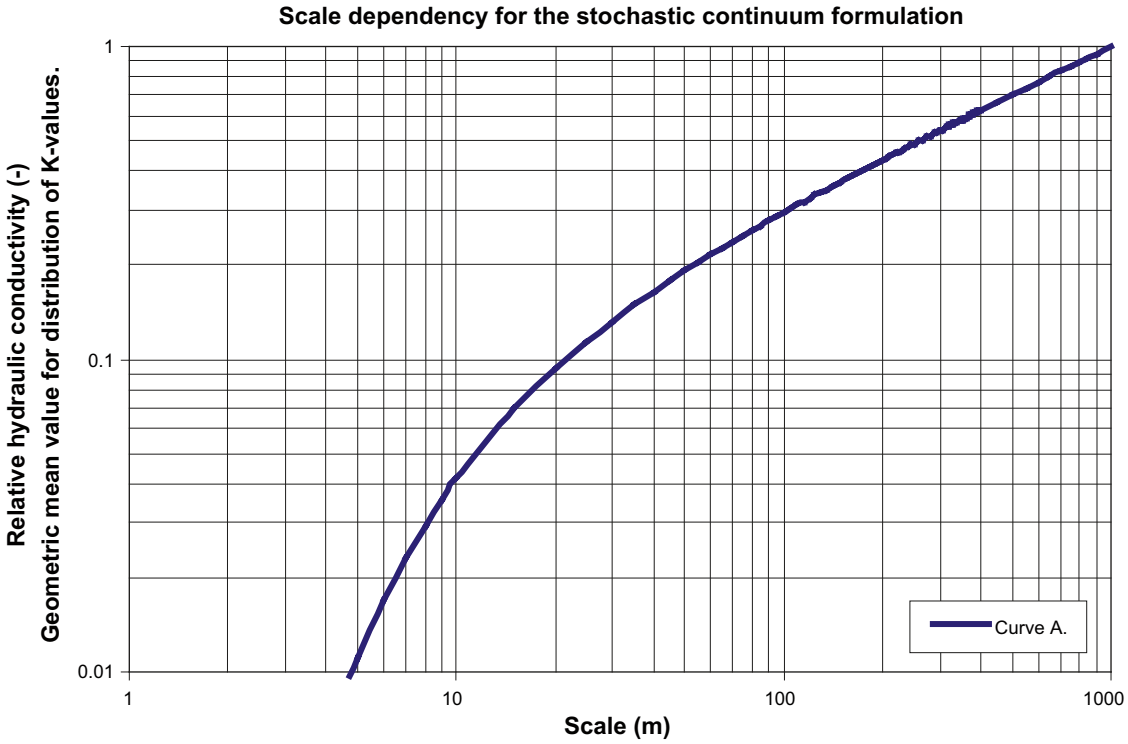

Figure A-1. *Local heterogeneity. Scale dependency in conductivity. Geometric mean conductivity at different scales. The values are given as relative values, relative to an effective value.*

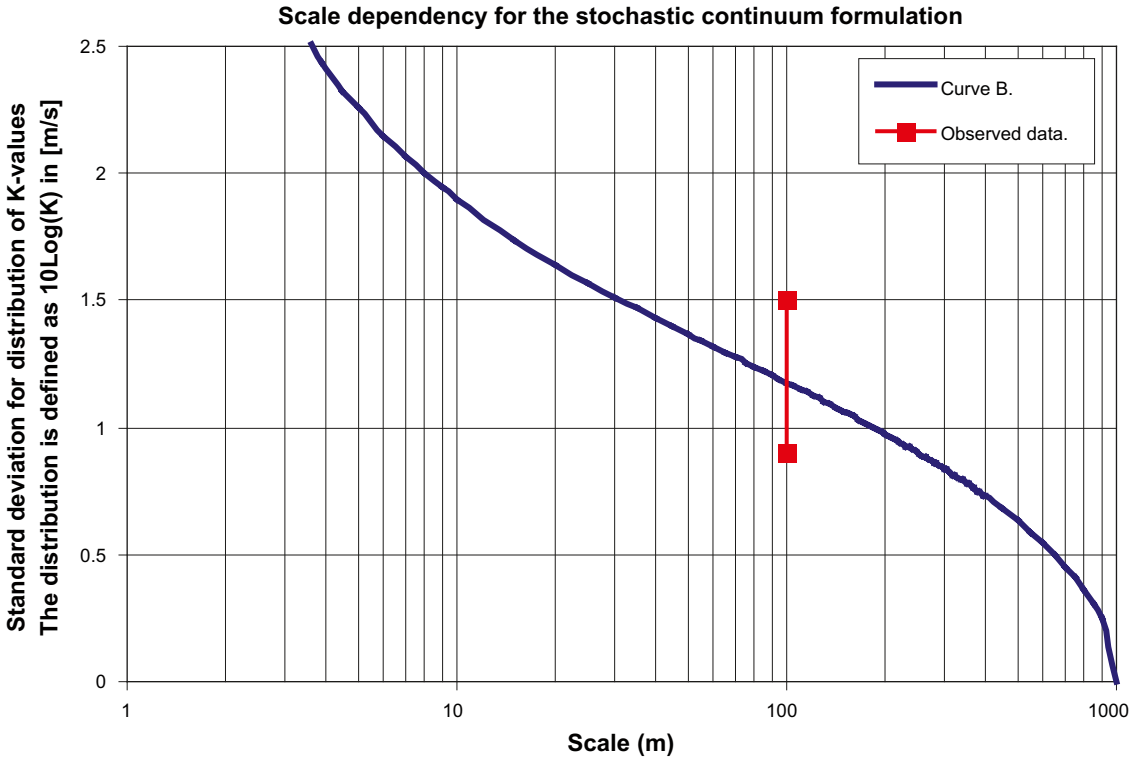

Figure A-2. *Local heterogeneity. Scale dependency in conductivity. Standard deviation (for 10Log values) at different scales.*